

# Magnetic Reconnection and Energy Conversions

A. Bhattacharjee

*Center for Heliophysics*

*Department of Astrophysical Sciences*

*Princeton Plasma Physics Laboratory*

*Princeton University*

*Acknowledgement: M. Yamada, PPPL*

LWS Heliophysics Summer School, July 25-August 3, 2016

## *What is Magnetic Reconnection?*

If a plasma is perfectly conducting, that is, it obeys the ideal Ohm's law,

$$\mathbf{E} + \mathbf{v} \times \mathbf{B}/c = 0$$

**B**-lines are frozen in the plasma, and no reconnection occurs.

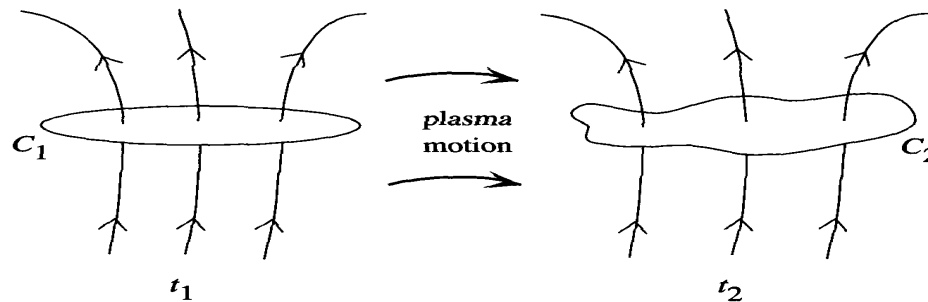


Fig. 1.6. Magnetic flux conservation: if a curve  $C_1$  is distorted into  $C_2$  by plasma motion, the flux through  $C_1$  at  $t_1$  equals the flux through  $C_2$  at  $t_2$ .

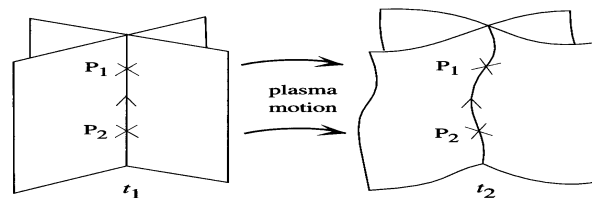


Fig. 1.7. Magnetic field-line conservation: if plasma elements  $P_1$  and  $P_2$  lie on a field line at time  $t_1$ , then they will lie on the same line at a later time  $t_2$ .

## *Magnetic Reconnection: Working Definition*

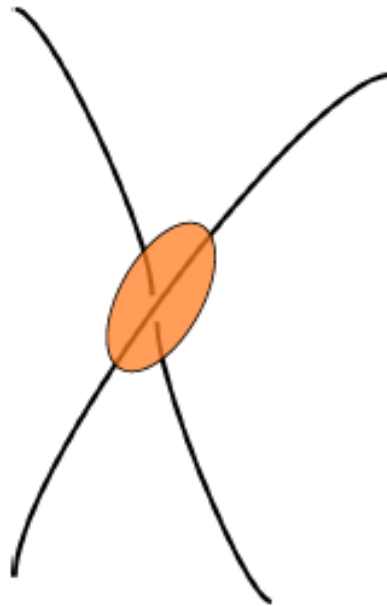
Departures from ideal behavior, represented by

$$\mathbf{E} + \mathbf{v} \times \mathbf{B} / c = \mathbf{R}, \quad \nabla \times \mathbf{R} \neq \mathbf{0}$$

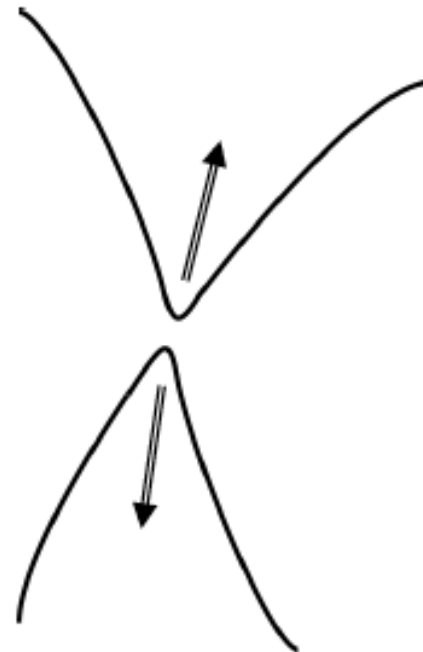
break ideal topological invariants, allowing field lines to break and reconnect.

In the generalized Ohm's law for weakly collisional or collisionless plasmas,  $\mathbf{R}$  contains resistivity, Hall current, electron inertia and pressure.

# Magnetic Reconnection



*Before reconnection*



*After reconnection*

- Topological rearrangement of magnetic field lines
- Magnetic energy  $\Rightarrow$  Kinetic energy

# *Example of Topological Change: Magnetic Island Formation*

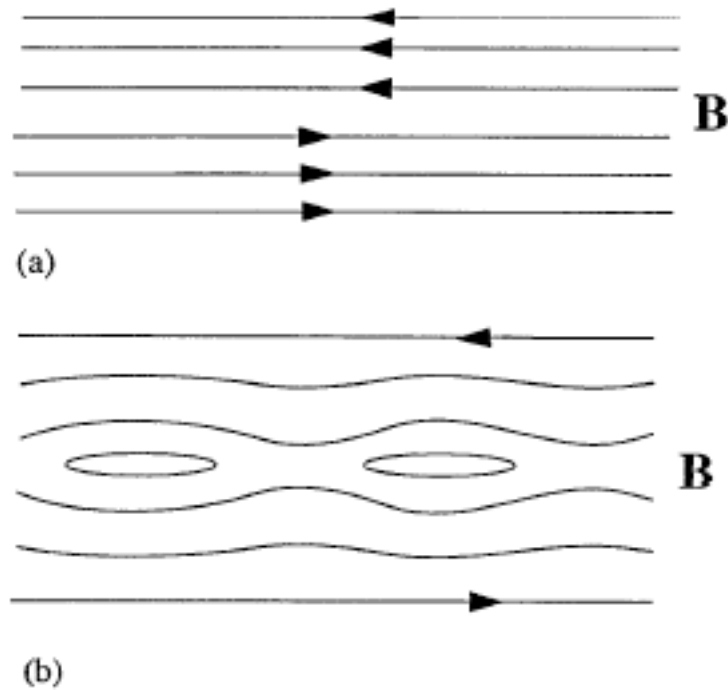
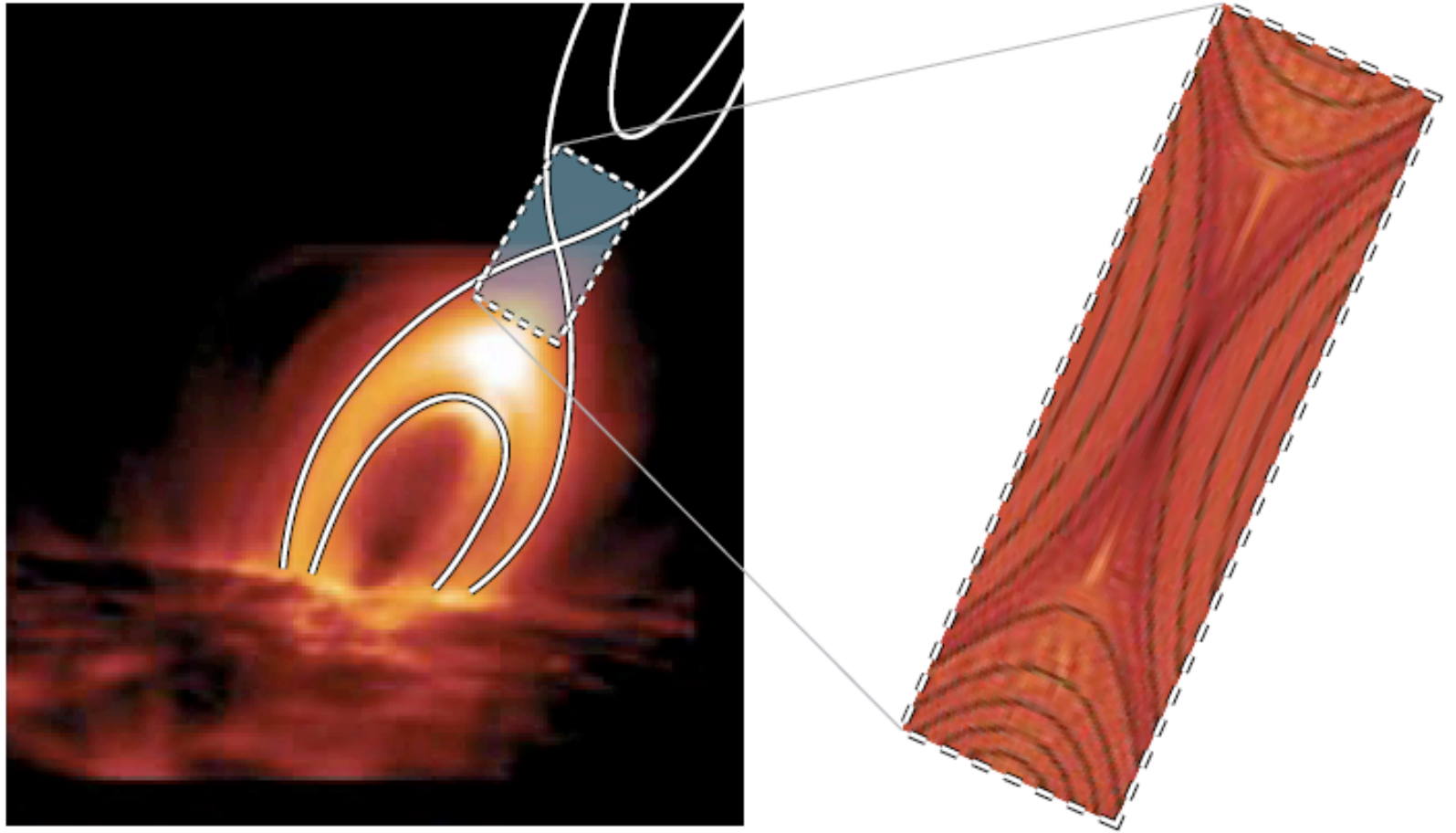


FIG. 1. (a) The topology of field lines in the Harris equilibrium  $\mathbf{B} = B_0 \tanh(z/a) \hat{\mathbf{x}}$ . (b) The topology of field lines when the perturbation  $\mathbf{h} = b \sin(kx) \hat{\mathbf{z}}$  is imposed on the Harris equilibrium.



*Courtesy: J. Burch and J. Drake, MMS Mission*

# A Coronal Mass Ejection

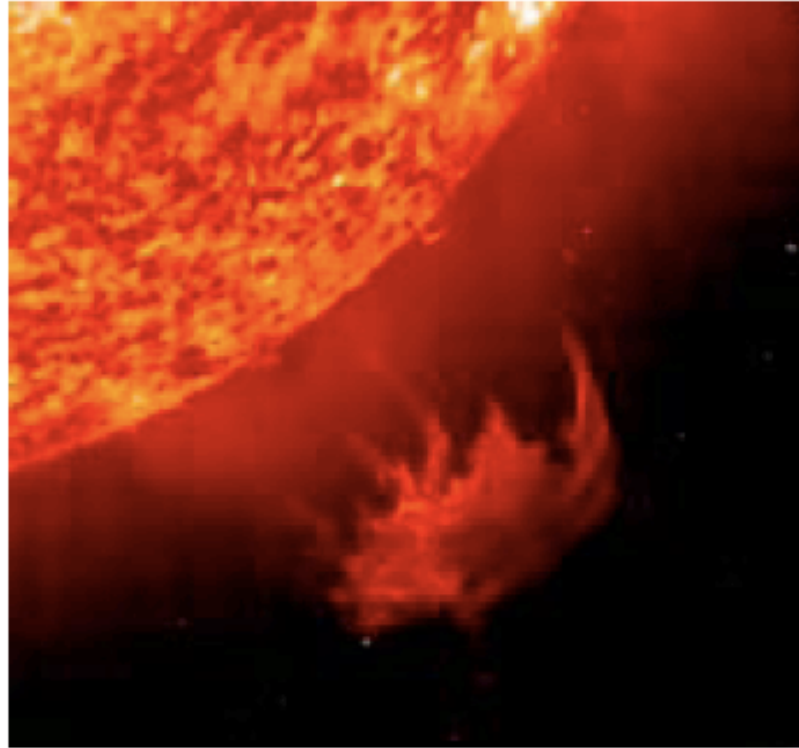



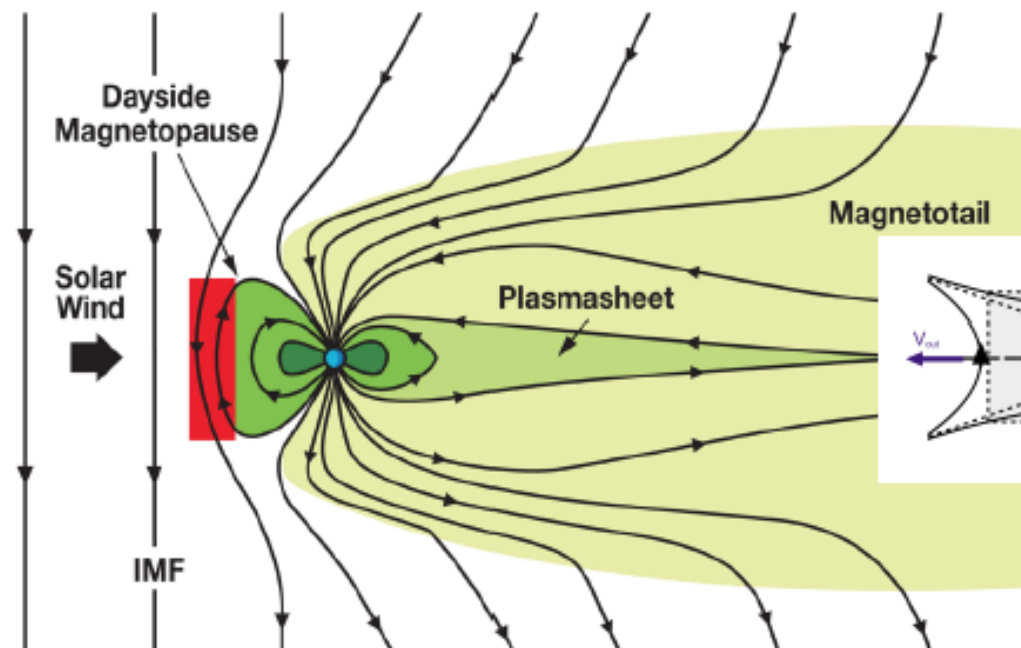
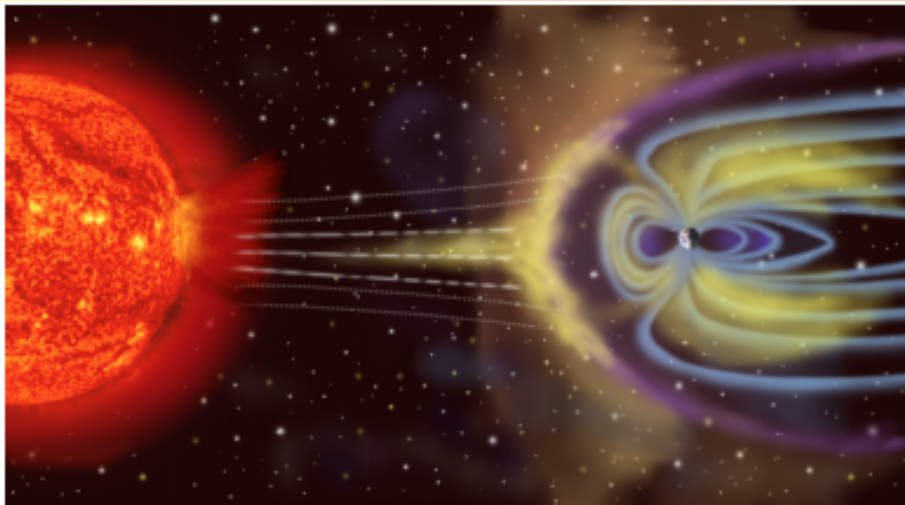
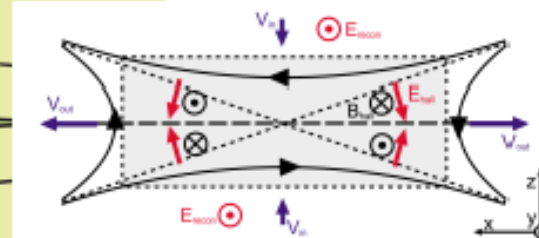
Image of a large eruption from the Sun when a large clump of solar mass is ejected into space, viewed from the satellite SOHO. On the scale of the image to the right, the Earth is the size of this blue sphere .

Image courtesy of SOHO.

# Magnetic reconnection layers in the magnetosphere



Data is available to evaluate inventory of energy flows

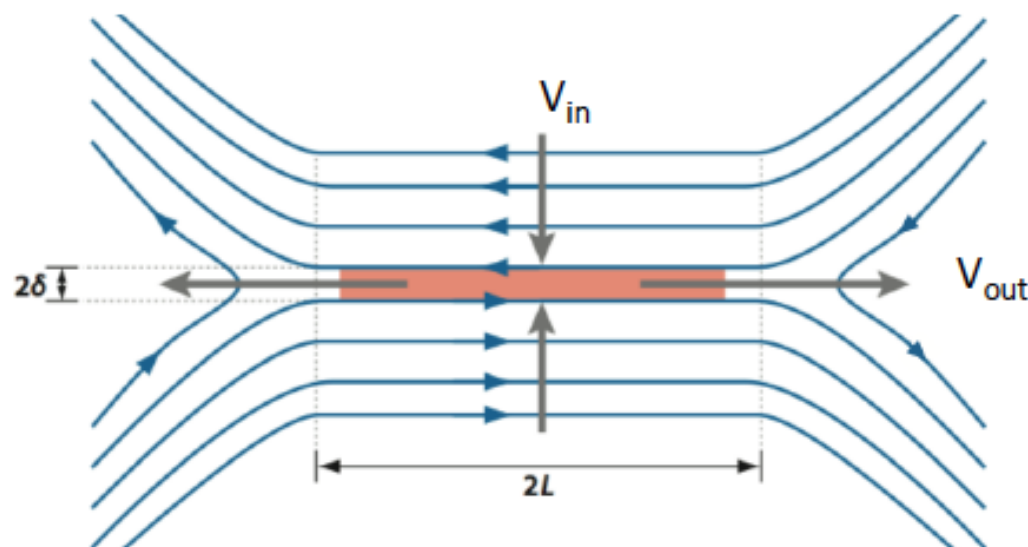




# The Sweet-Parker Model for Magnetic Reconnection

Assume;

- 2D
- Steady-state
- Incompressibility
- Classical Spitzer resistivity



$$\frac{\partial \mathbf{B}}{\partial t} = \nabla \times (\mathbf{v} \times \mathbf{B}) + \frac{\eta}{\mu_0} \nabla^2 \mathbf{B} \quad \Rightarrow \quad V_{in} B = \frac{\eta_{Spitz}}{\mu_0} \frac{B}{\delta} \quad \Rightarrow \quad \boxed{\frac{V_{in}}{V_A} = \frac{1}{\sqrt{S}}}$$

Mass conservation:

$$V_{in} L \approx V_{out} \delta$$

$$S = \frac{\mu_0 L V_A}{\eta_{Spitz}}$$

Pressure balance:

$$\frac{1}{2} \rho V_{out}^2 \approx \frac{B^2}{2\mu_0} \Rightarrow V_{out} \approx V_A$$

$S$  = Lundquist number

In solar flares,  $\tau_{SP} \sim 1 \text{ year} \gg \tau_{reconn}$

Q. Why is Sweet-Parker reconnection so slow?

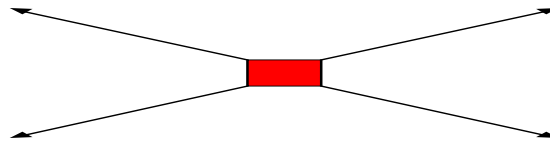
A. Geometry

Conservation relations of mass, energy, and flux

$$V_{in}L = V_{out}\delta, \quad V_{out} = V_A$$

$$V_{in} = \frac{\delta}{L}V_A, \quad \frac{\delta}{L} = S^{-1/2}$$

Petschek [1964]



Geometry of reconnection layer: X-point

Length  $\Delta$  ( $\ll L$ ) is of the order of the width  $\delta$

$$\tau_{PK} = \tau_A \ln S$$

Solar flares:  $\tau_{PK} \sim 10^2 s$

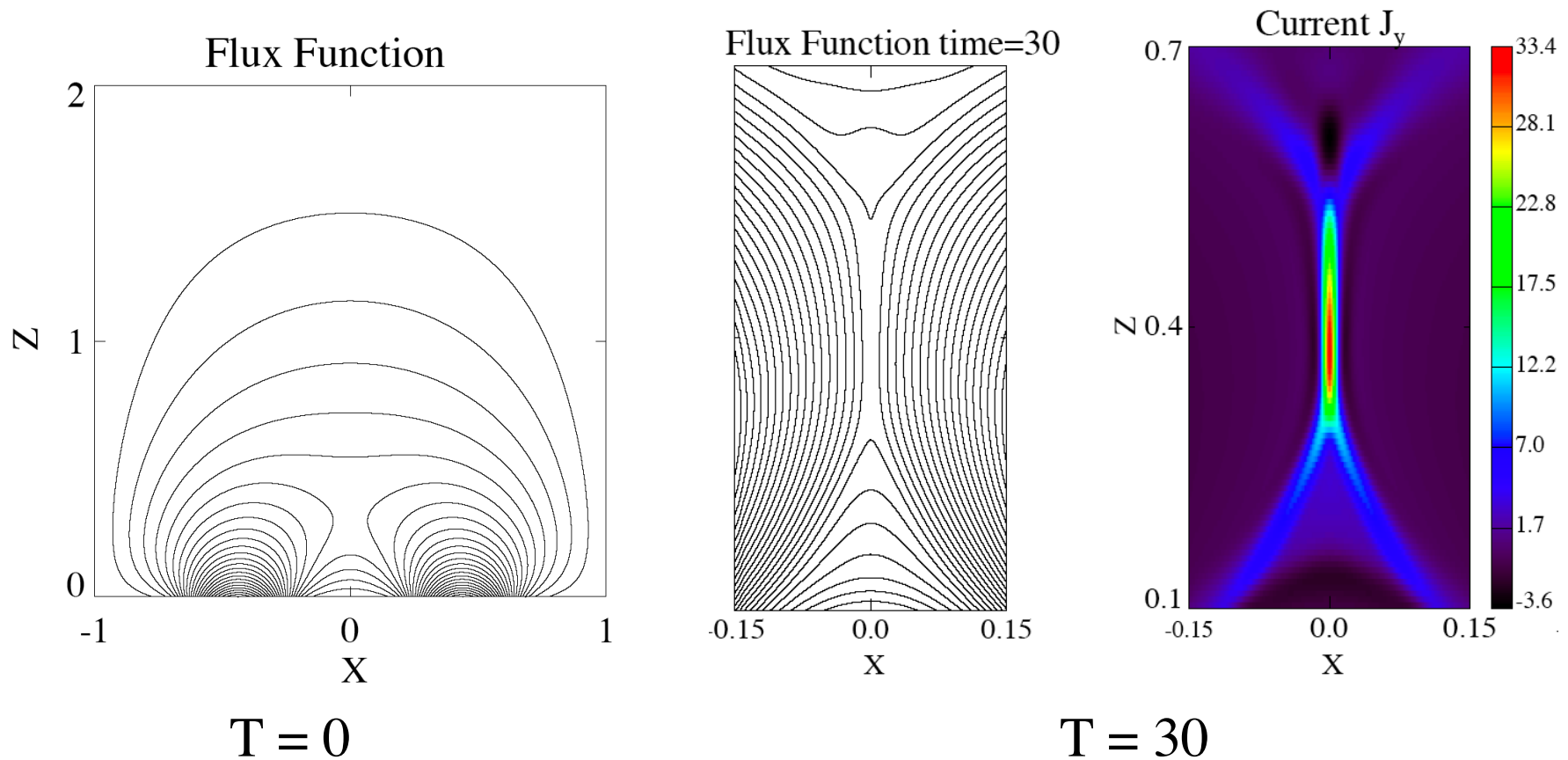
## *Computational Tests of the Petschek Model*

[Sato and Hayashi 1979, Ugai 1984, Biskamp 1986, Forbes and Priest 1987, Scholer 1989, Yan, Lee and Priest 1993, Ma et al. 1995, Uzdensky and Kulsrud 2000, Breslau and Jardin 2003, Malyshkin, Linde and Kulsrud 2005]

### *Conclusions*

- Petschek model is not realizable in high-S plasmas, unless the resistivity is locally strongly enhanced at the X-point.
- In the absence of such anomalous enhancement, the reconnection layer evolves dynamically to form Y-points and realize a Sweet-Parker regime.

## 2D coronal loop : high-Lundquist number resistive MHD simulation



[Ma, Ng, Wang, and Bhattacharjee 1995]

## Impulsive Reconnection: The Onset/Trigger Problem

Dynamics exhibits an impulsiveness, that is, a sudden change in the time-derivative of the reconnection rate.

The magnetic configuration evolves slowly for a long period of time, only to undergo a sudden dynamical change over a much shorter period of time.

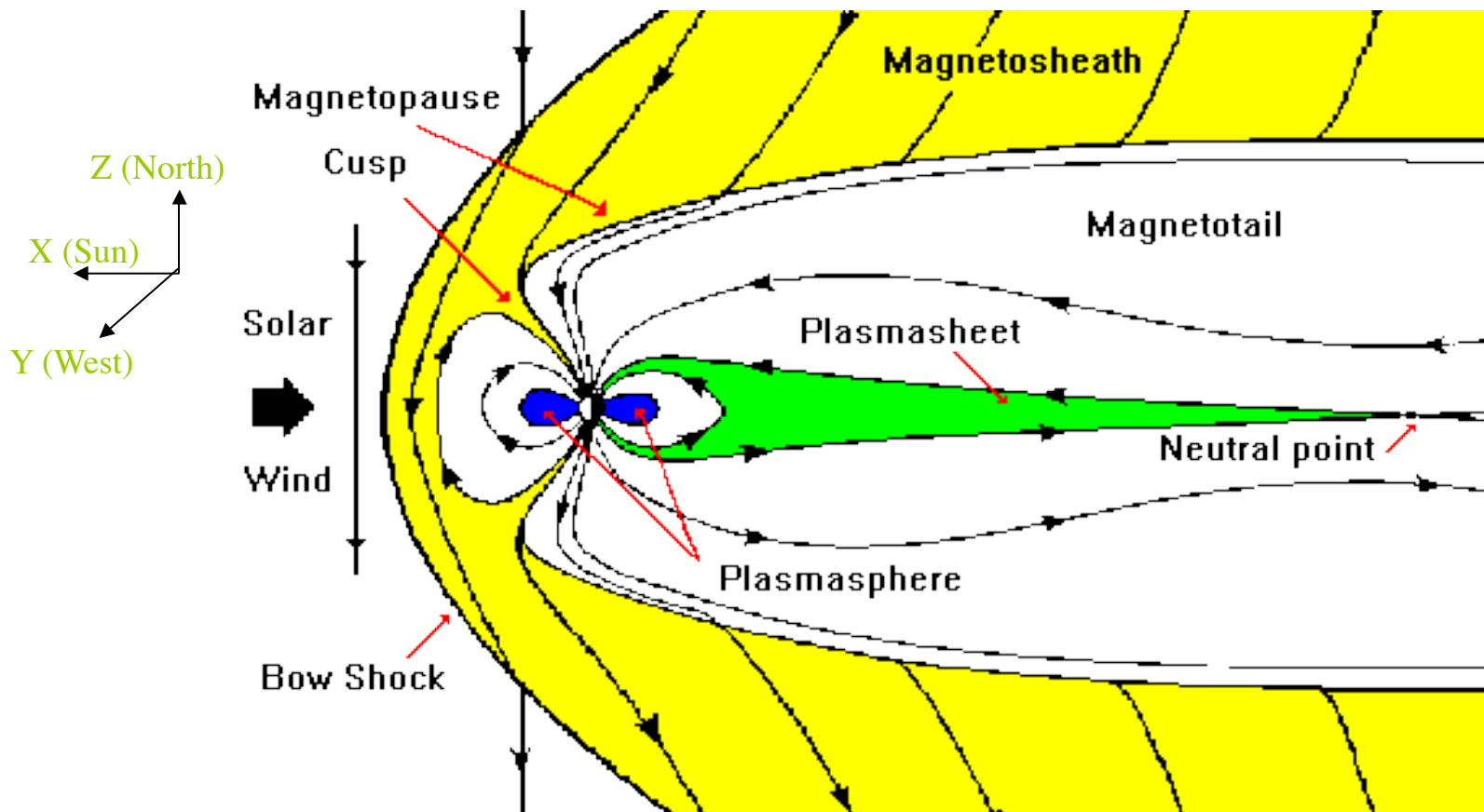
Dynamics is characterized by the formation of near-singular current sheets which need to be resolved in computer simulations: a classic multi-scale problem coupling large scales to small.

### *Examples*

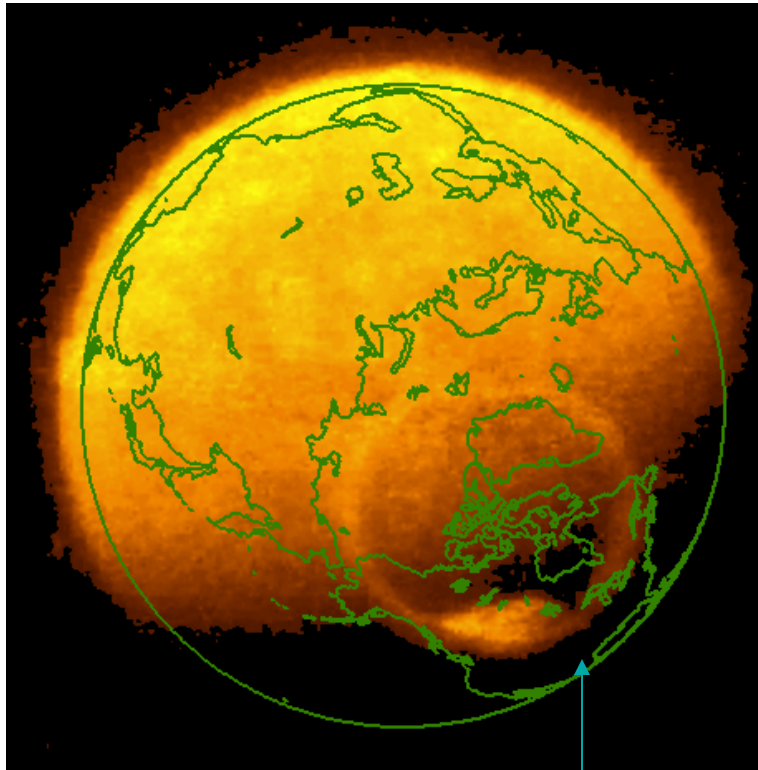
#### **Magnetospheric substorms**

Impulsive solar/stellar flares

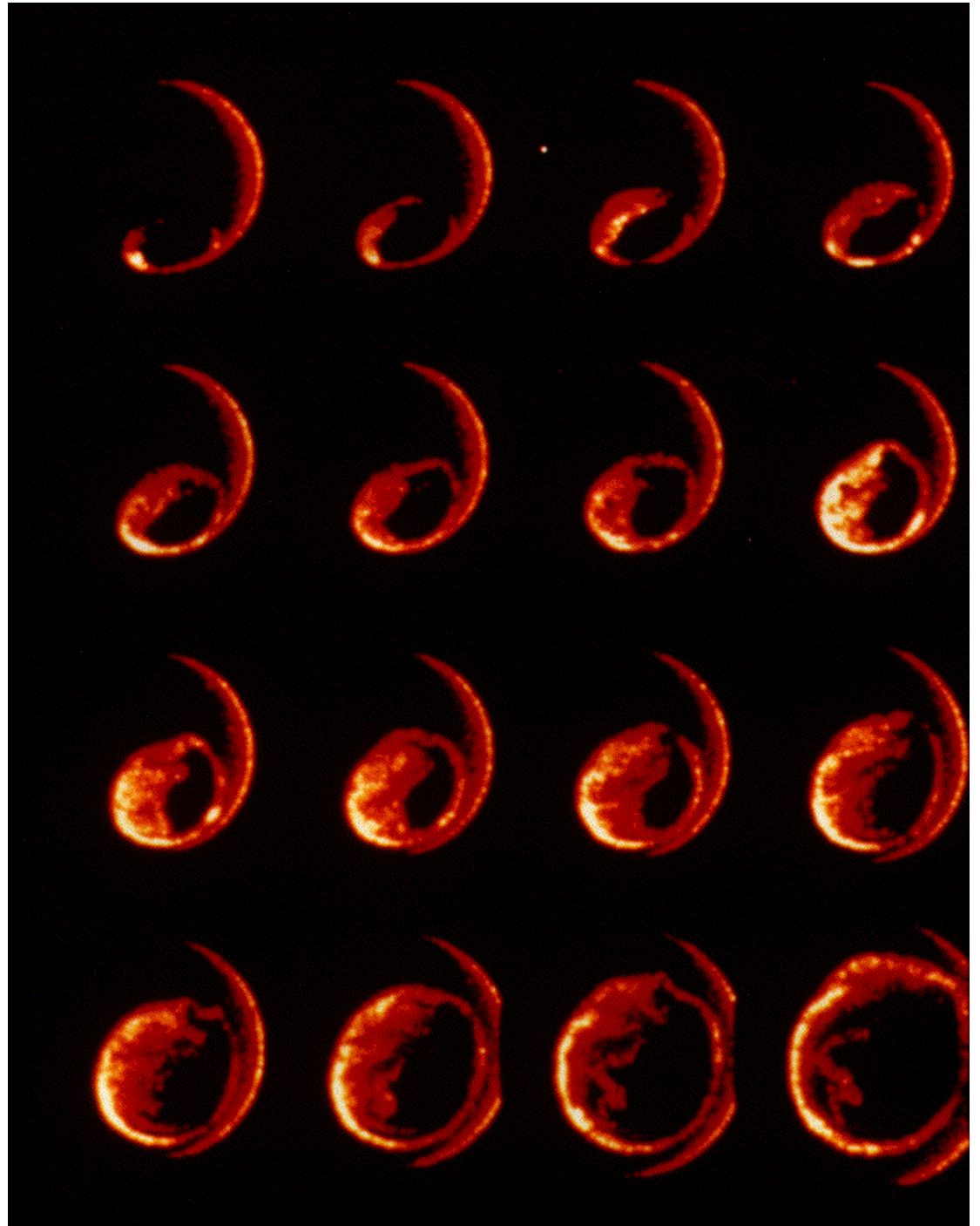
## Substorm Onset: Where does it occur?



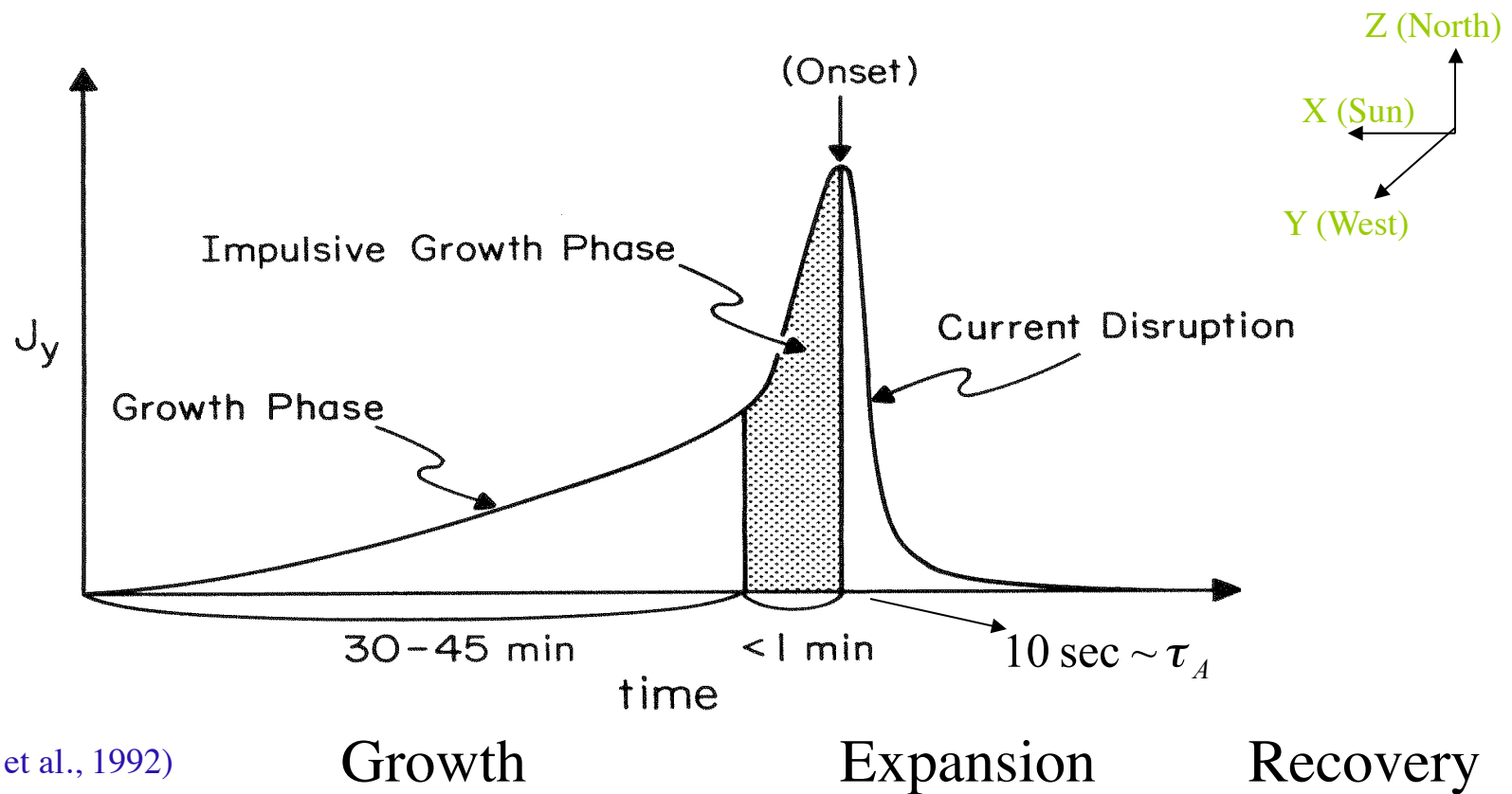
## Substorm Onset:



Auroral bulge



# Substorm Onset: When does it occur?





# Generalized Ohm's law

What's really important?

$$\mathbf{E} = \underbrace{-\mathbf{v}_i \times \mathbf{B}}_{(i)} - \underbrace{\frac{m_e}{e} \frac{d\mathbf{v}_e}{dt}}_{(ii)} - \underbrace{\frac{1}{en_e} \nabla \cdot \vec{P}_e}_{(iii)} + \underbrace{\frac{1}{en_e} \mathbf{J} \times \mathbf{B}}_{(iv)} + \underbrace{\eta_e \mathbf{J}}_{(v)}$$

$$\frac{(i)}{(v)} = \frac{vB}{\eta_e B / \mu_0 \ell} = \frac{\ell v \mu_0}{\eta_e} \equiv R_m$$

$$\frac{(i)}{(ii)} = \frac{vB}{m_e v B / \mu_0 e^2 n_e \ell^2} = \frac{\ell^2}{m_e / \mu_0 e^2 n_e} = \left( \frac{\ell}{c / \omega_{pe}} \right)^2$$

$$\frac{(i)}{(iv)} = \frac{vB}{B^2 / \mu_0 en_e \ell} = \frac{v\ell}{B / \mu_0 en_e} = \left( \frac{v}{v_A} \right) \left( \frac{\ell}{c / \omega_{pi}} \right)$$

$$\frac{(i)}{(iii)} = \frac{vB}{p_e / en_e \ell} = \frac{v\ell}{k_B T / e B} = \left( \frac{v}{c_s} \right) \left( \frac{\ell}{\rho_i} \right)$$

Importance of term depends on length scale of solution

**On large scales plasma is ideal conductor\***

\* except where  $\mathbf{B}=0$

# Hall MHD (or Extended MHD) Model and the Generalized Ohm's Law

In high- $S$  plasmas, when the width of the thin current sheet ( $\Delta_\eta$ ) satisfies

$$\Delta_\eta < c / \omega_{pi} \quad (\text{or } \rho_s \equiv \sqrt{\beta} c / \omega_{pi} \text{ if there is a guide field})$$

“collisionless” terms in the generalized Ohm's law cannot be ignored.

Generalized Ohm's law (dimensionless form)

$$\mathbf{E} + \mathbf{v} \times \mathbf{B} = \frac{1}{S} \mathbf{J} + d_e^2 \frac{d\mathbf{J}}{dt} + \frac{d_i}{n} (\mathbf{J} \times \mathbf{B} - \nabla p_e)$$

Electron skin depth

$$d_e \equiv L^{-1} (c / \omega_{pe})$$

Ion skin depth

$$d_i \equiv L^{-1} (c / \omega_{pi})$$

Electron beta

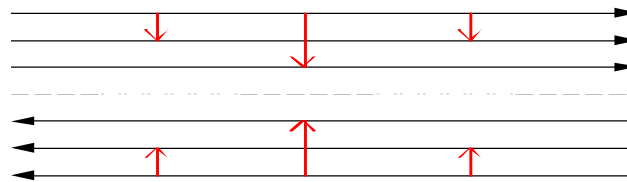
$$\beta_e$$

## Onset of fast reconnection in large, high-Lundquist-number systems

- As the original current sheet thins down, it will inevitably reach kinetic scales, described by a generalized Ohm's law (including Hall current and electron pressure gradient).
- A criterion has emerged from Hall MHD (or two-fluid) models, and has been tested carefully in laboratory experiments (MRX at PPPL, VTF at MIT). The criterion is:  
 $\delta_{SP} < d_i$  (Ma and Bhattacharjee 1996, Cassak et al. 2005) or  $\delta_{SP} < \rho_s$  in the presence of a guide field (Aydemir 1992; Wang and Bhattacharjee 1993; Kleva, Drake and Waelbroeck 1995)

# Forced Magnetic Reconnection Due to Inward Boundary Flows

Magnetic field



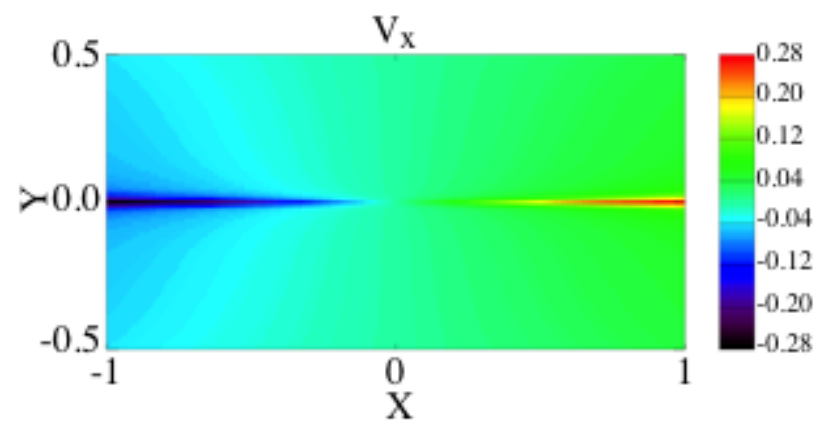
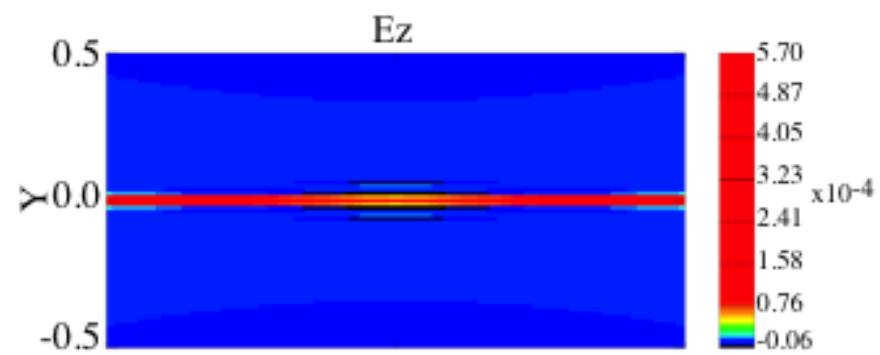
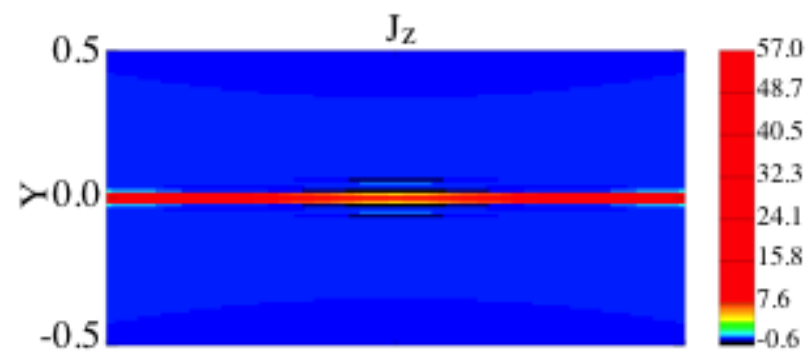
$$\mathbf{B} = \hat{\mathbf{x}}B_P \tanh z/a + \hat{\mathbf{z}}B_T$$

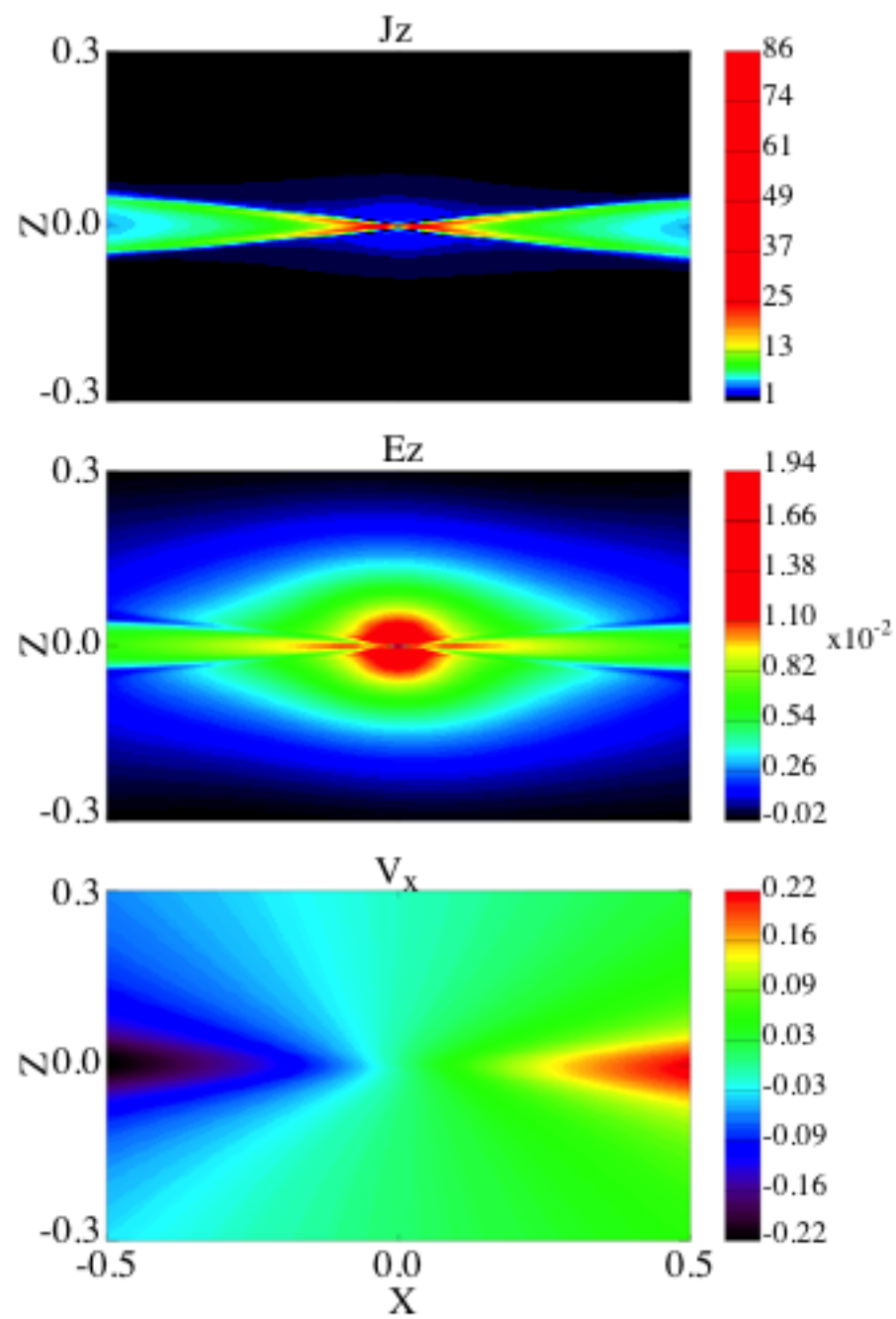
Inward flows at the boundaries

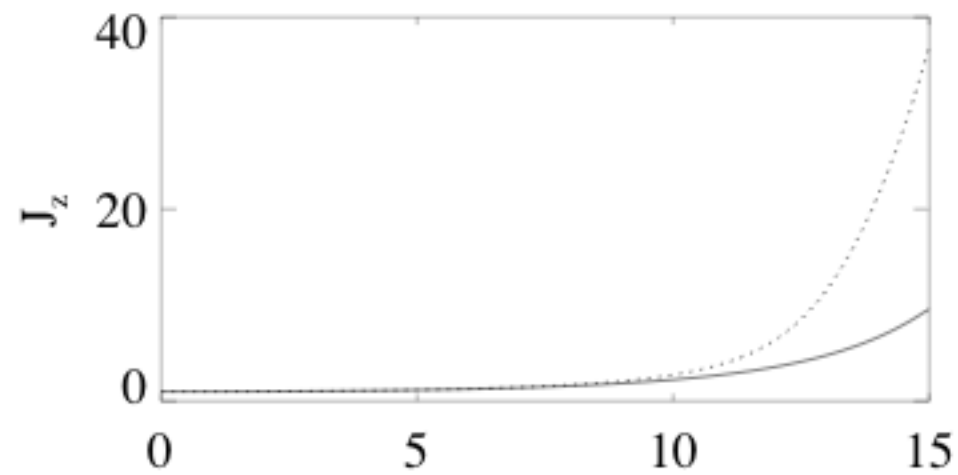
$$\mathbf{v} = \mp V_0(1 + \cos kx)\hat{\mathbf{y}}, \quad \Delta' < 0$$

Two simulations: Resistive MHD versus Hall MHD [Ma and Bhattacharjee 1996]

For other perspectives, with similar conclusions, see Grasso et al. (1999) Dorelli and Birn (2003), Fitzpatrick (2004), Cassak et al. (2005), Simakov and Chacon (2008), Malyshkin (2008)

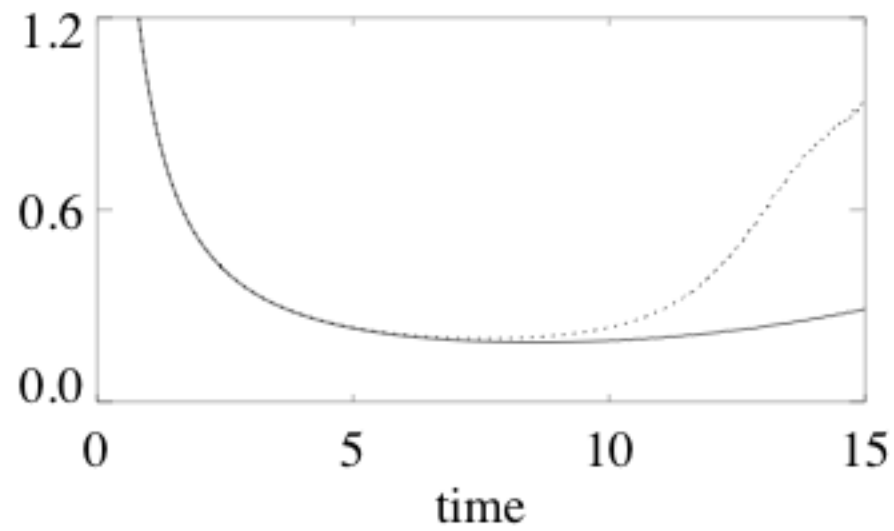


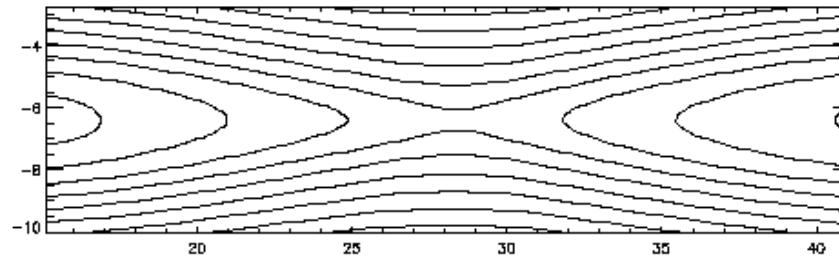




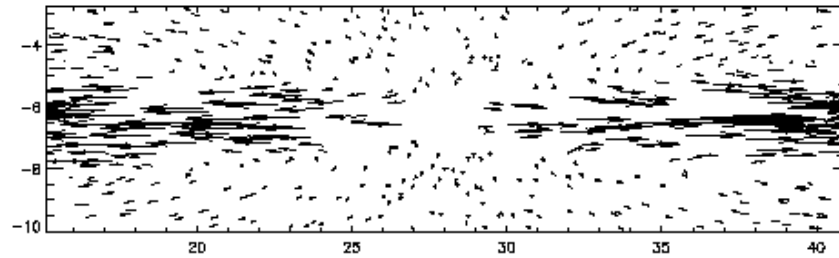
..... Hall  
 \_\_\_\_ Resistive

$d \ln \psi / dt$

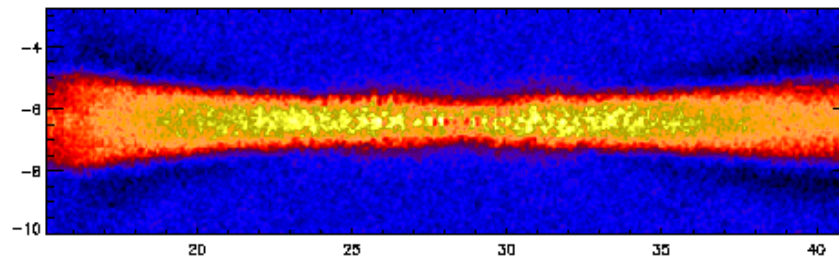




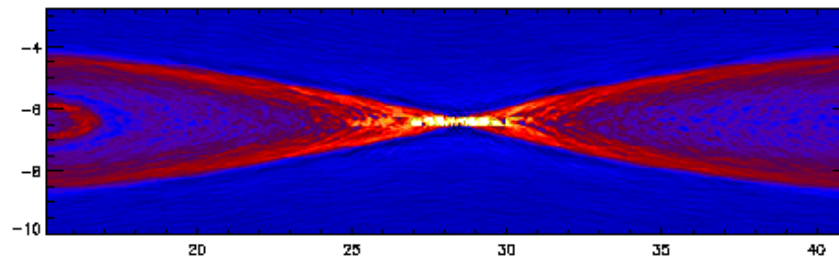
Field lines



Electron flows



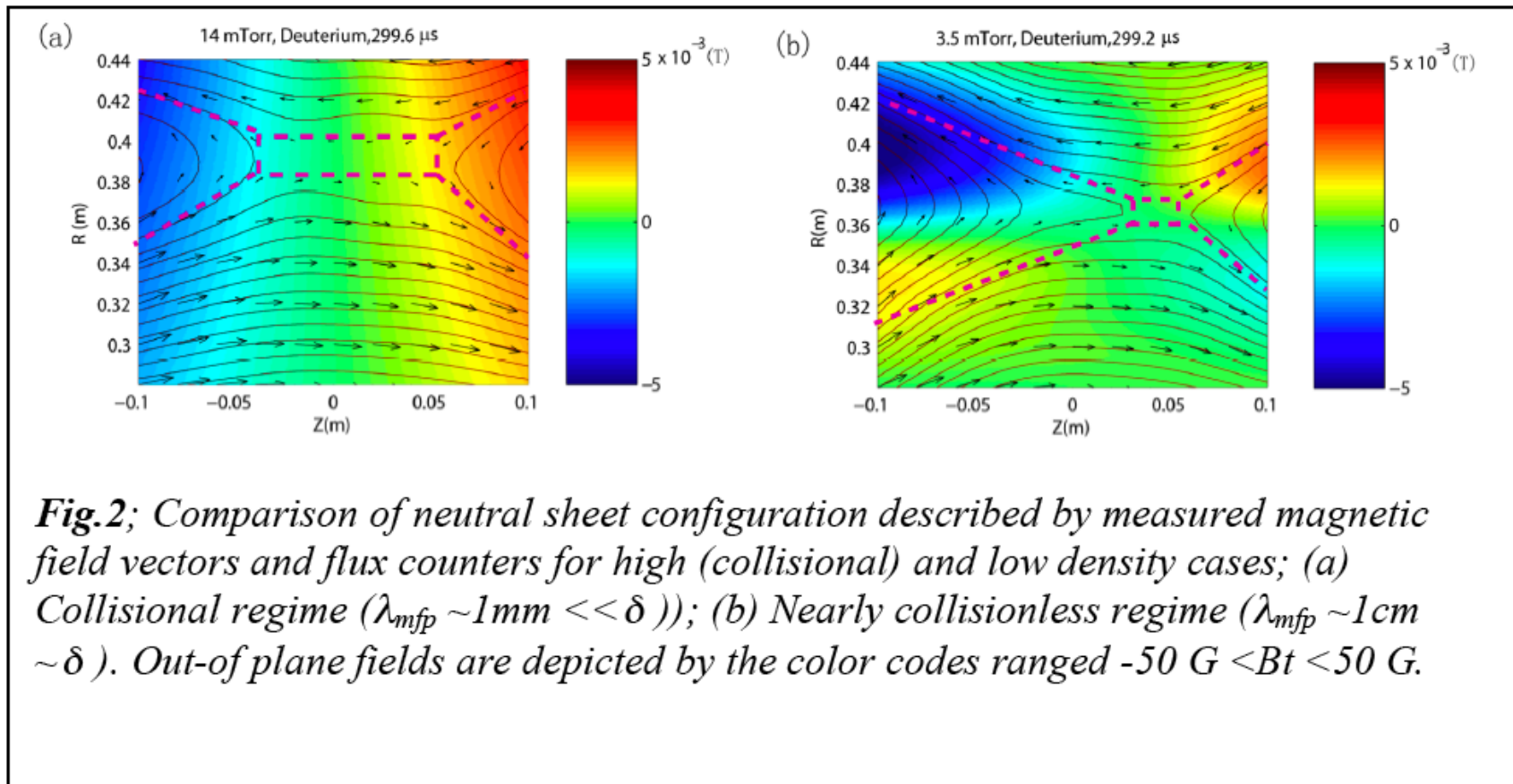
Ion current density



Electron current density



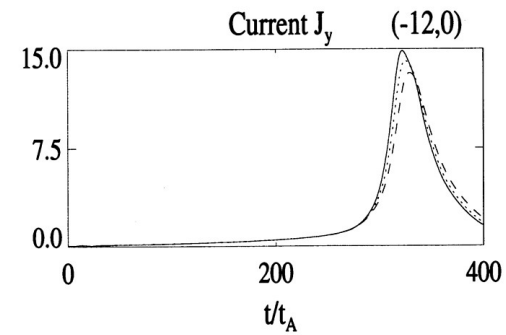
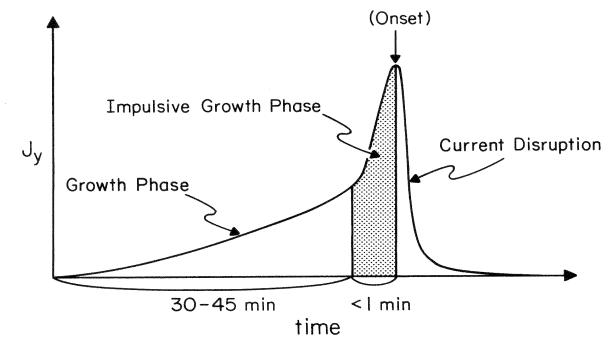
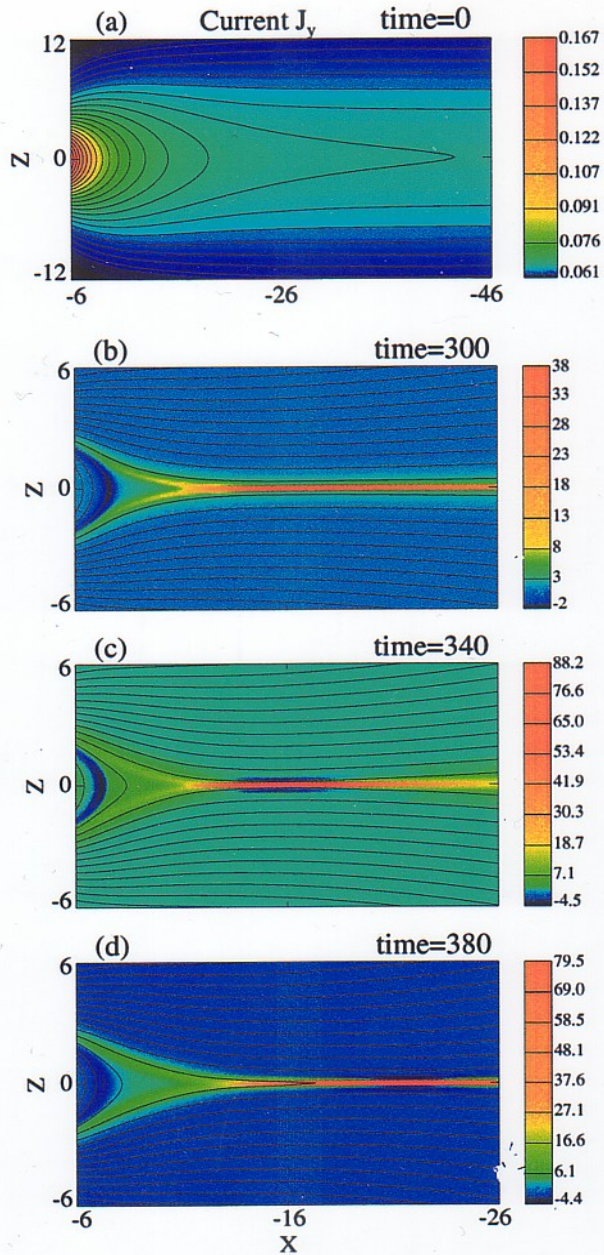
## Transition from Collisional to Collisionless Regimes in MRX



## Linkage between space and laboratory plasmas

System	L (cm)	B (G)	$d_i = c/\omega_{pi}$ (cm)	$\delta_{sp}$ (cm)	$d_i / \delta_{sp}$
MRX	10	100-500	1-5	0.1-5	.2-100
Tokamak	100	$10^4$	10	0.1	100
Magnetosphere	$10^9$	$10^{-3}$	$10^7$	$10^4$	1000
Solar flare	$10^9$	100	$10^4$	$10^2$	100
ISM	$10^{18}$	$10^{-6}$	$10^7$	$10^{10}$	0.001
Proto-star	$d_i / \delta_s \gg 1$				

$$d_i / \delta_{sp} \sim 5(\lambda_{mfp}/L)^{1/2}$$

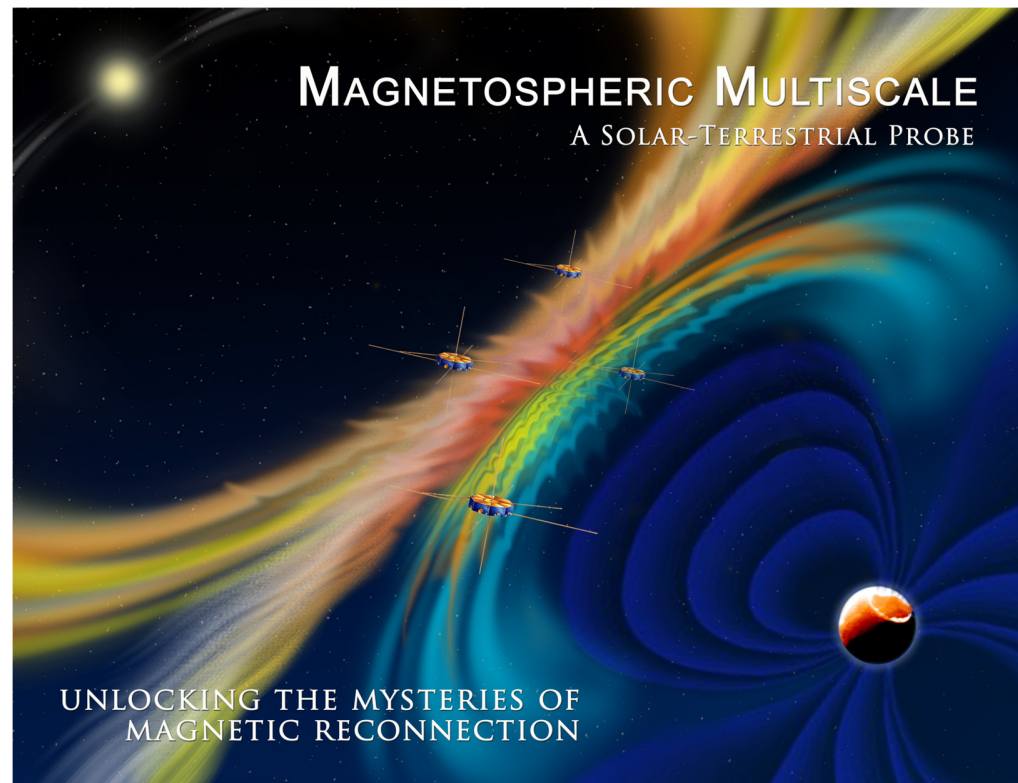


## 2D Hall-MHD Simulation (Ma and Bhattacharjee, 1998)

# Magnetospheric Multiscale Mission

- The MMS Mission science will be conducted by the SMART (Solving Magnetospheric Acceleration, Reconnection and Turbulence) Instrument Suite Science Team and a group of three Interdisciplinary Science (IDS) teams.
- Launched 2015.

<http://mms.space.swri.edu>



*(Courtesy: J. Burch, SWRI)*

# Plasmoid Instability of *Large-Scale* Current Sheets

## Sweet-Parker (Sweet 1958, Parker 1957)



Geometry of reconnection layer : Y-points (Syrovatsky 1971)

Length of the reconnection layer is of the order of the system size  $\gg$  width  $\Delta$

Reconnection time scale

$$\tau_{SP} = (\tau_A \tau_R)^{1/2} = S^{1/2} \tau_A$$

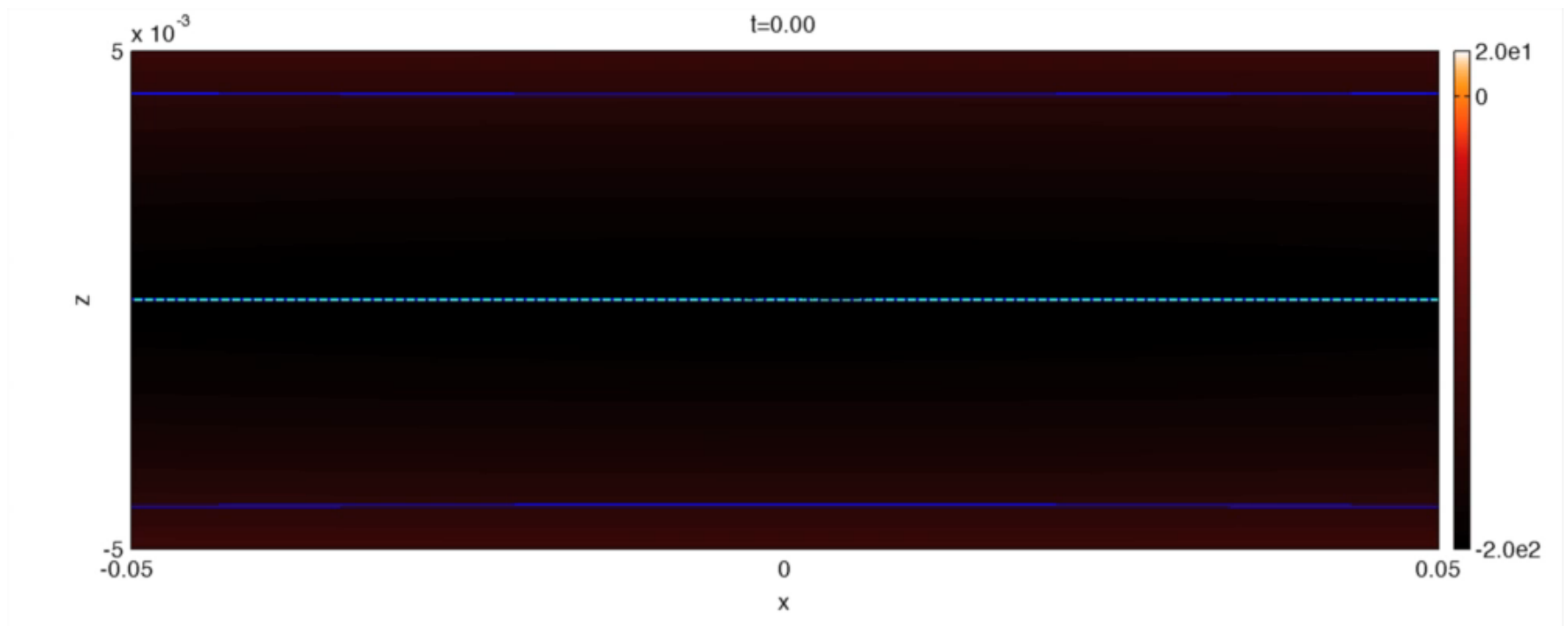
Solar flares:  $S \sim 10^{12}$ ,  $\tau_A \sim 1s$

$$\Rightarrow \tau_{SP} \sim 10^6 s \quad \text{Too long!}$$

## Fast Reconnection in Large Systems

- Extended thin current sheets of high Lundquist number are unstable to a super-Alfvenic tearing instability ([Loureiro et al. 2007](#)), which we call the “plasmoid instability,” because it generates a large number of plasmoids.
- In the nonlinear regime, the reconnection rate becomes nearly independent of the Lundquist number, and is much larger than the Sweet-Parker rate.

The thin current sheet is explosively stable if we exceed a critical Lundquist number,  $S_c$  forming, ejecting, and coalescing a hierarchy of plasmoids.



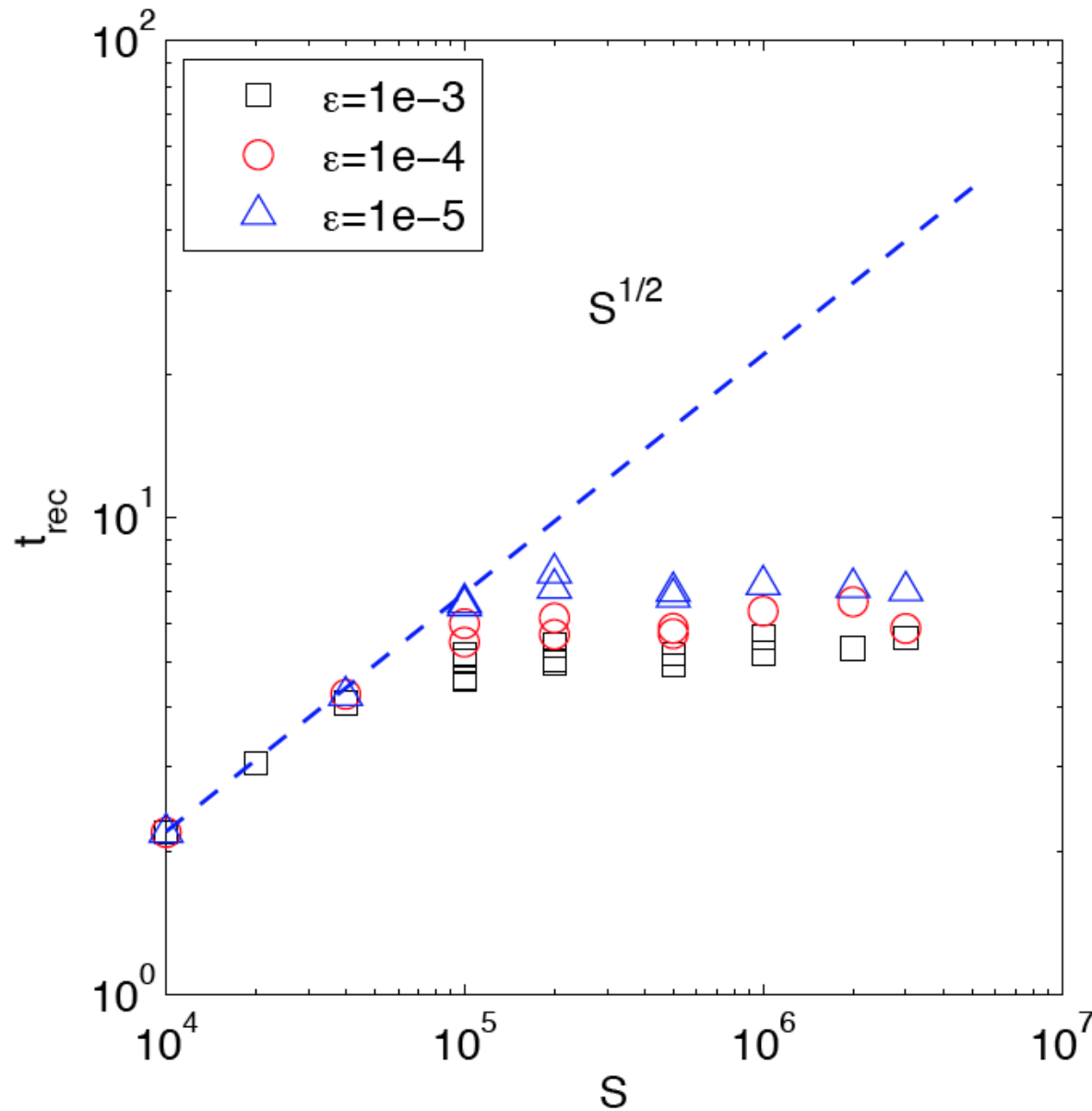
Bhattacharjee et al. 2009, Huang and Bhattacharjee 2010,  
Uzdensky et al. 2010



## A little history

- Secondary tearing instability of high-S current sheet has been known for some time (Bulanov et al. 1979, Lee and Fu 1986, Biskamp 1986, Matthaeus and Lamkin 1986, Yan et al. 1992, Shibata and Tanuma 2001), but its precise scaling properties were determined only recently.
- The instability has been studied recently nonlinearly in fluid (Lapenta 2008, Cassak et al. 2009; Samtaney et al. 2009) as well as fully kinetic studies with a collision operator (Daughton et al. 2009).

## Reconnection Time of 25% of Initial Flux



$$\left\langle \frac{1}{V_A B} \frac{d\psi}{dt} \right\rangle \sim 0.01$$

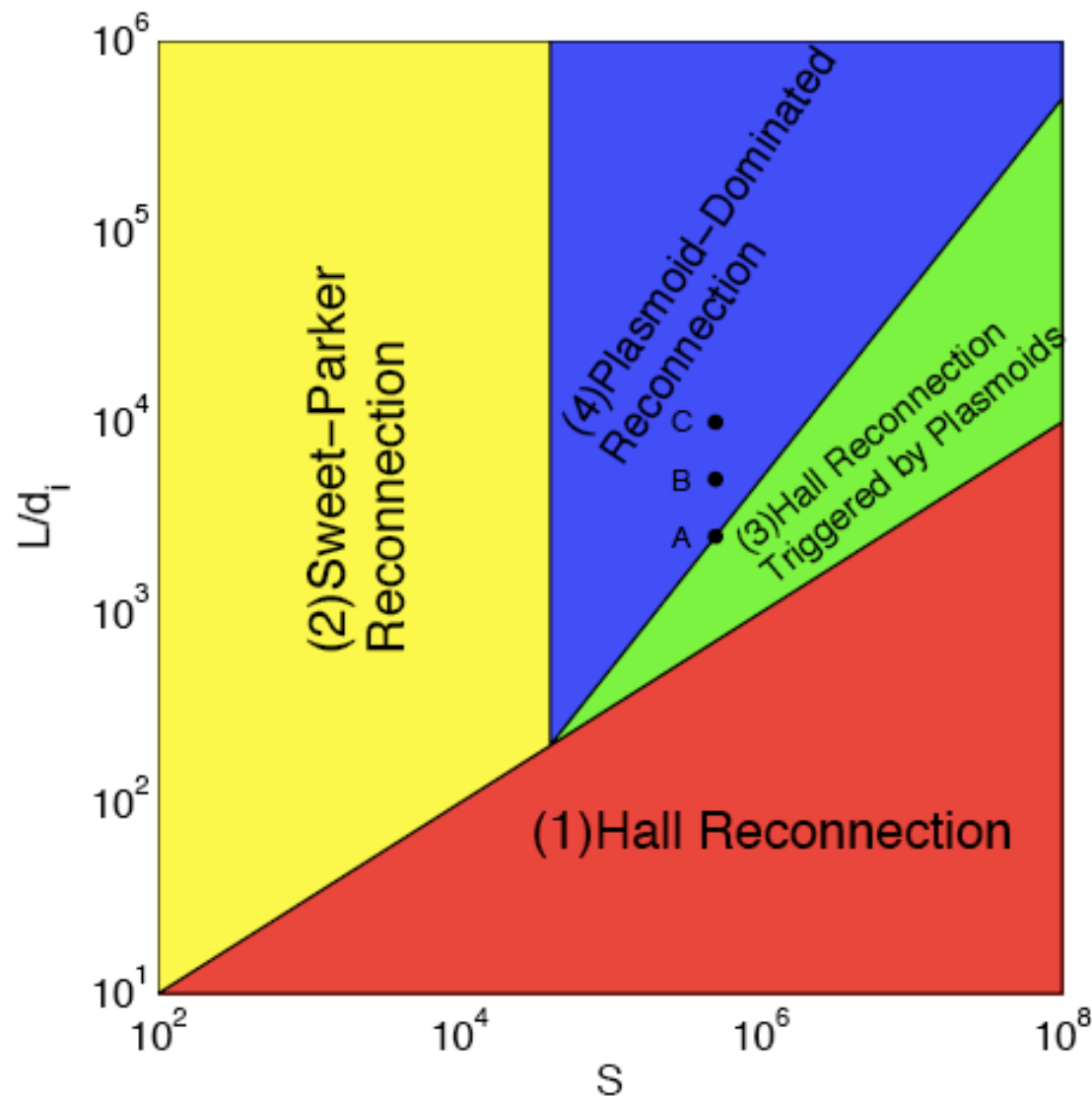
$$\langle u_i \rangle \sim 0.01 V_A$$

# Heuristic Scaling Argument Based on Marginal Stability

- Cascade to smaller scales will stop when local current sheets become stable to the plasmoid instability
- New plasmoids are generated when local current sheets exceed a critical length.
- Consider the reconnection layer as a chain of plasmoids connected by marginally stable current sheets. For a critical Lundquist number  $S_c$ :
  - Critical length  $L_c \sim S_c \eta / V_A \sim LS_c / S$
  - Number of plasmoids  $n_p \sim L / L_c \sim S / S_c$
  - Current sheet with  $\delta_c \sim L_c / S_c^{1/2} \sim LS_c^{1/2} / S$
  - Current density  $J \sim B / \delta_c \sim BS / LS_c^{1/2}$
  - Reconnection rate  $\sim \eta J \sim \eta B / \delta_c \sim BV_A / S_c^{1/2}$ , which is independent of  $S$

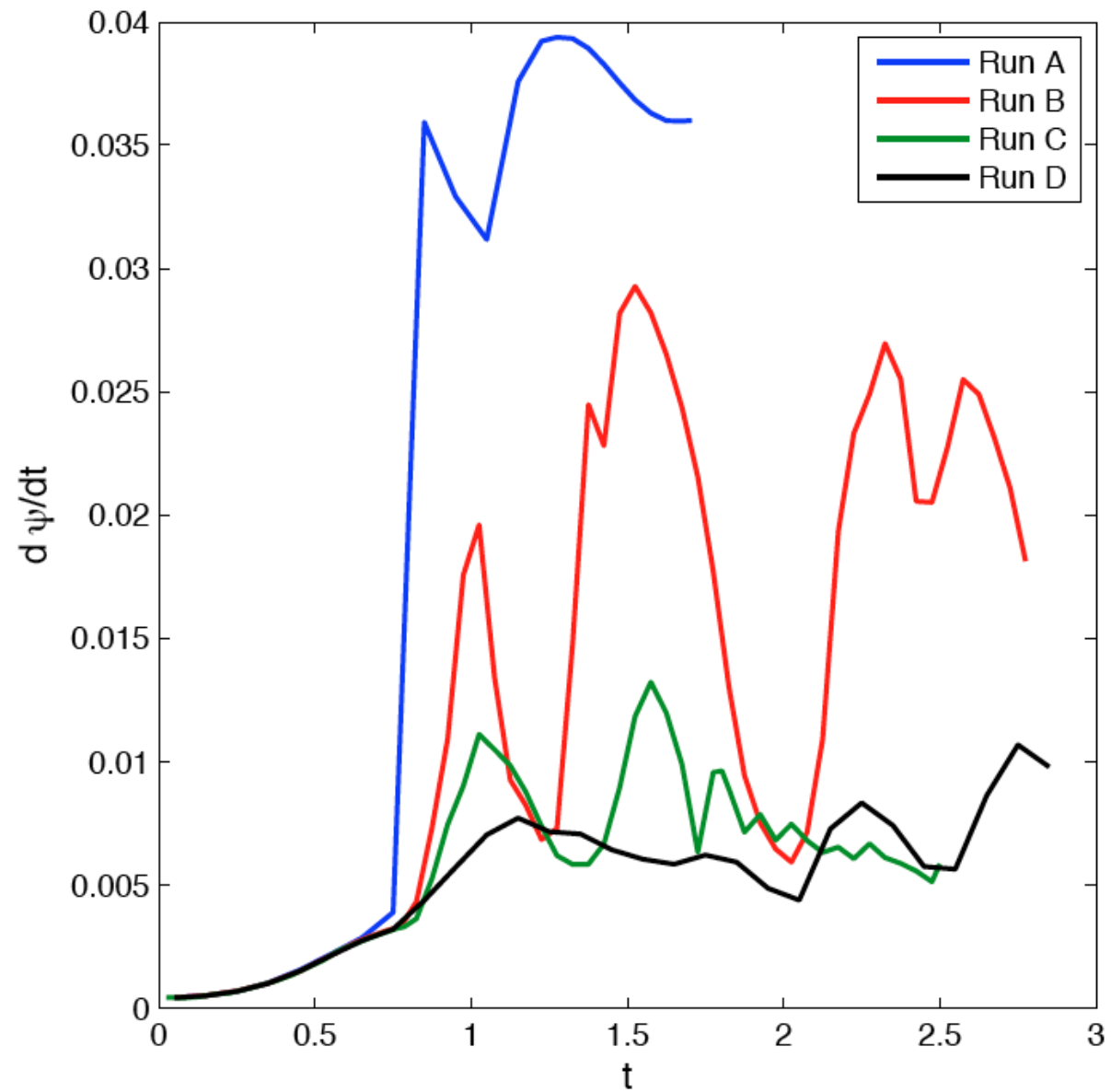


# Parameter Space

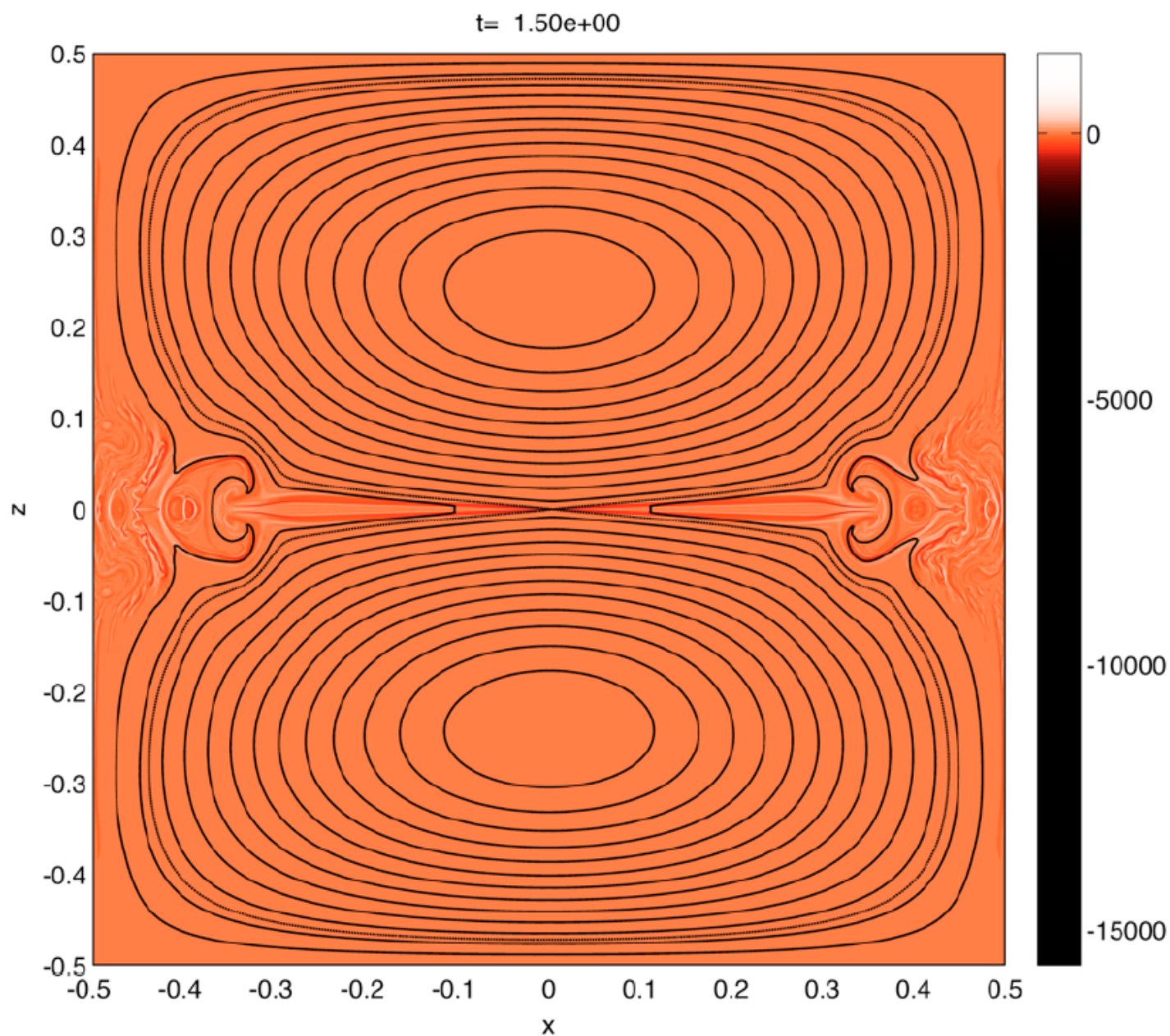


- A:  $S = 5 \times 10^5, d_i = 4 \times 10^{-4}$   
 B:  $S = 5 \times 10^5, d_i = 2 \times 10^{-4}$   
 C:  $S = 5 \times 10^5, d_i = 10^{-4}$   
 D:  $S = 5 \times 10^5, d_i = 0$

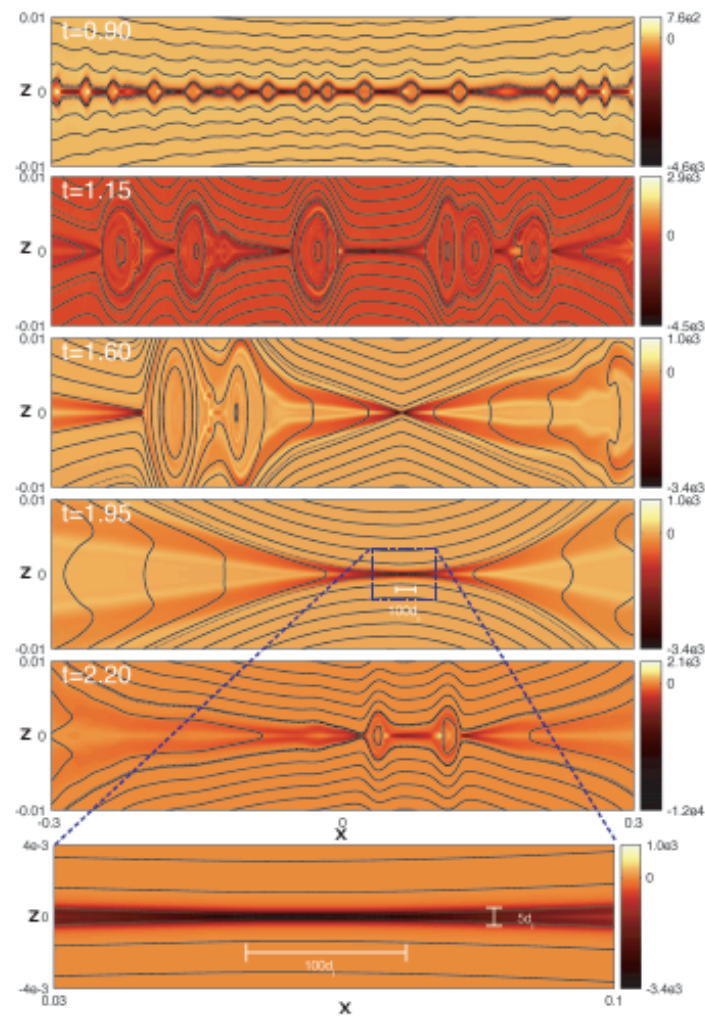
# Reconnection Rate



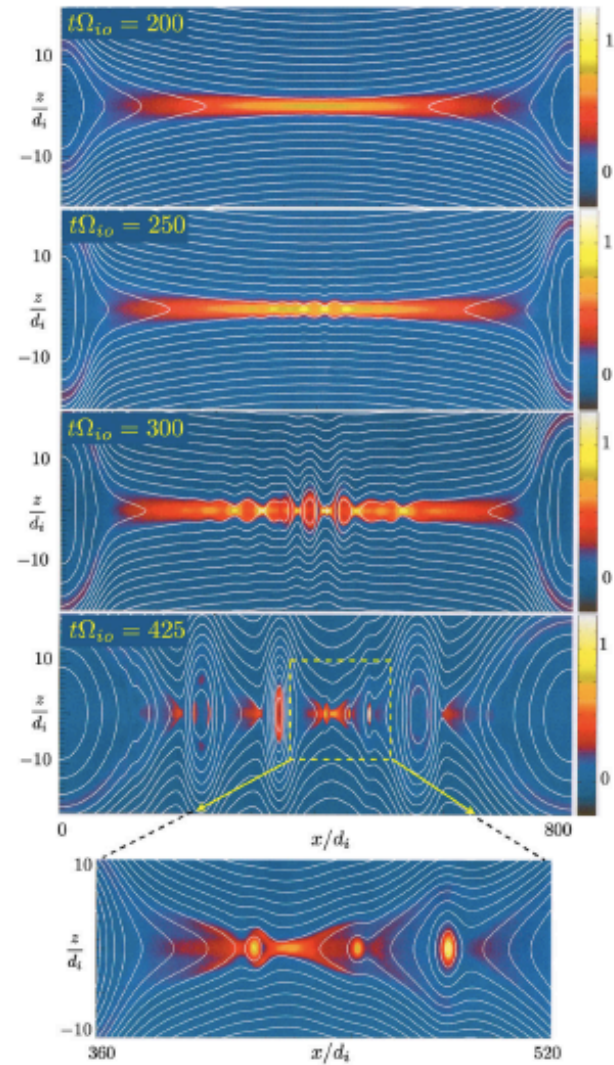
# Run A, global configuration at late time







Run B, resistive Hall

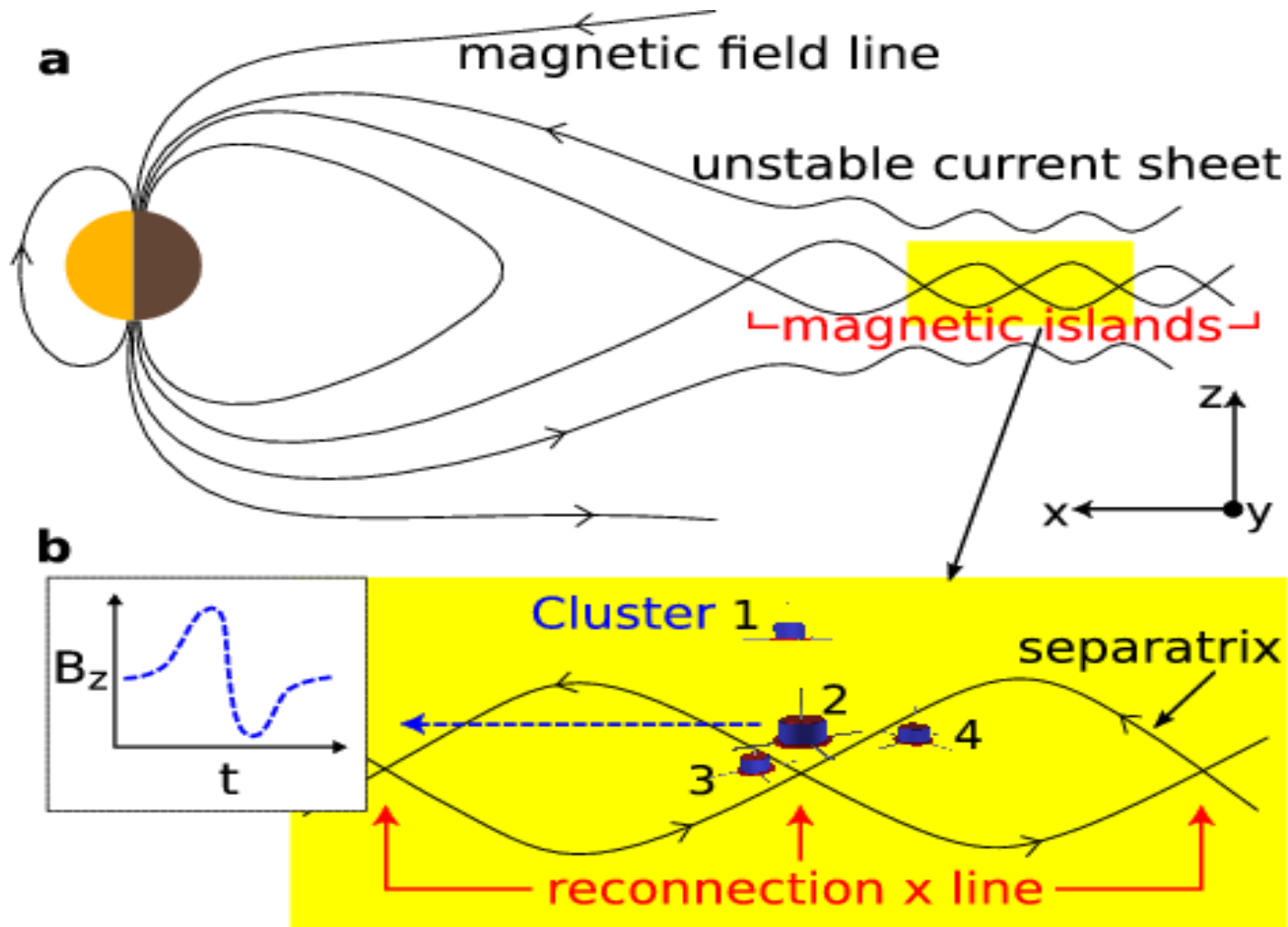


Daughton et al. (2009), PIC

Largest 2D Hall MHD simulation to date

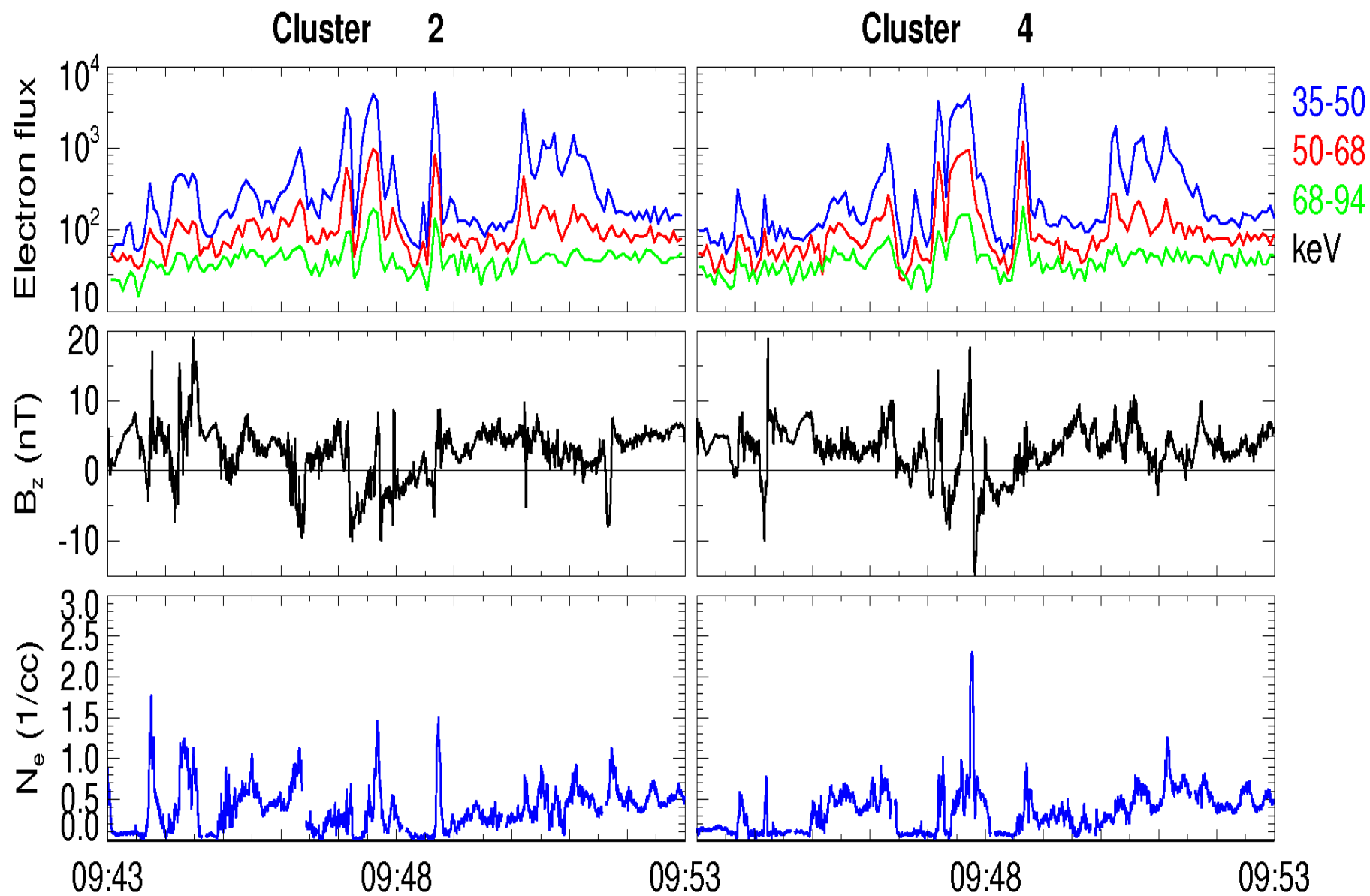
# Observations of energetic electrons within magnetic islands

[Chen et al., Nature Phys., 2008, PoP 2009]

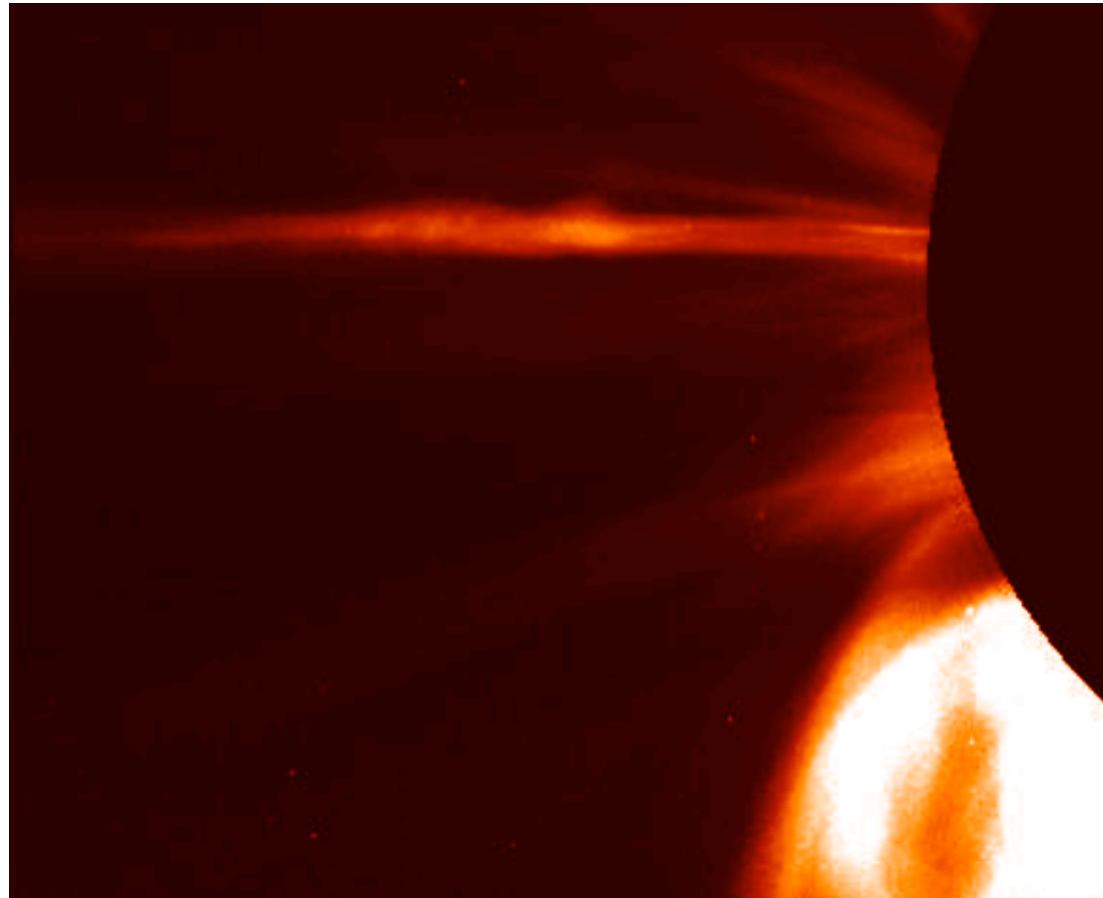




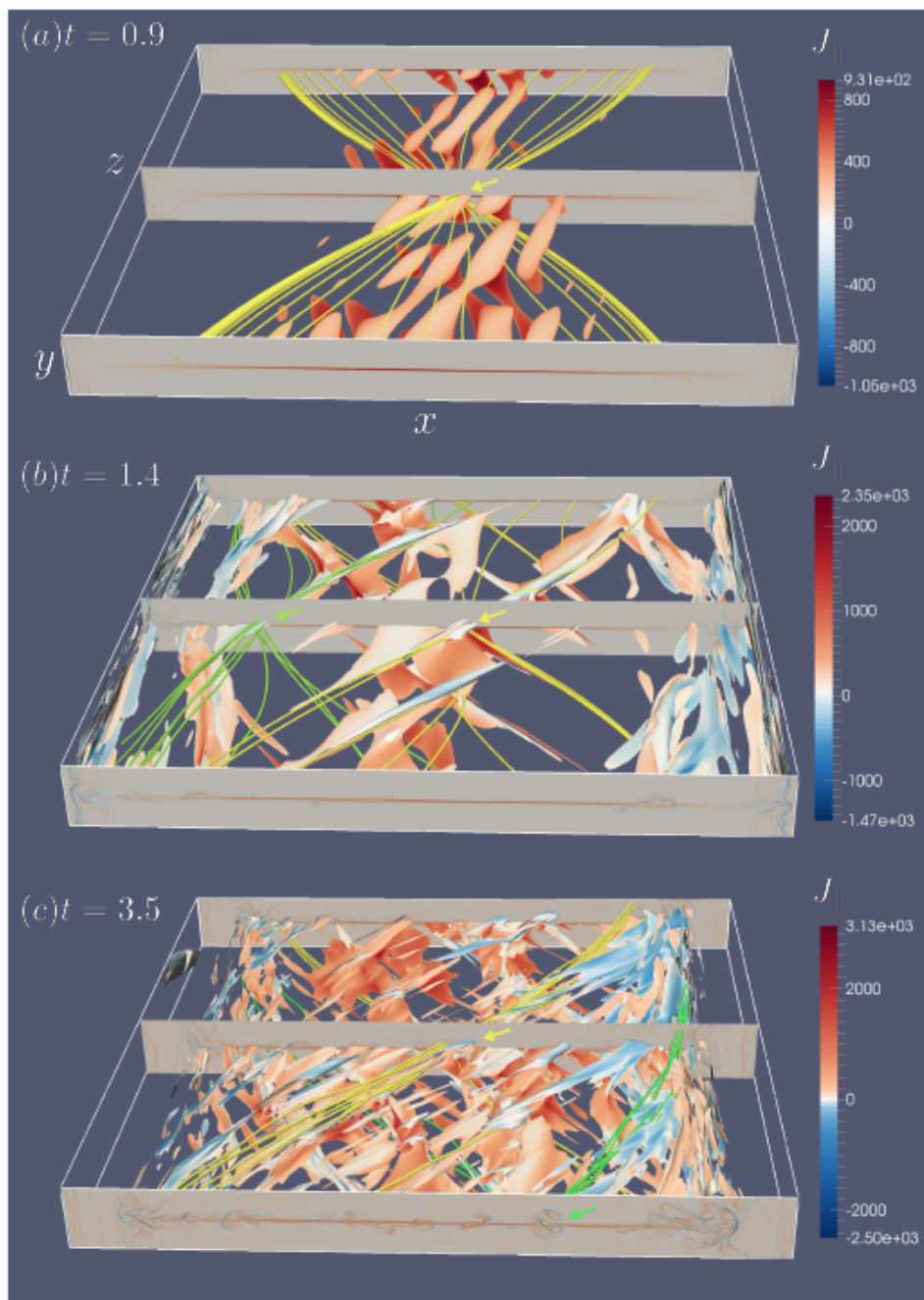
e bursts & bipolar Bz & Ne peaks  
~10 islands within 10 minutes



## Post CME Current Sheet

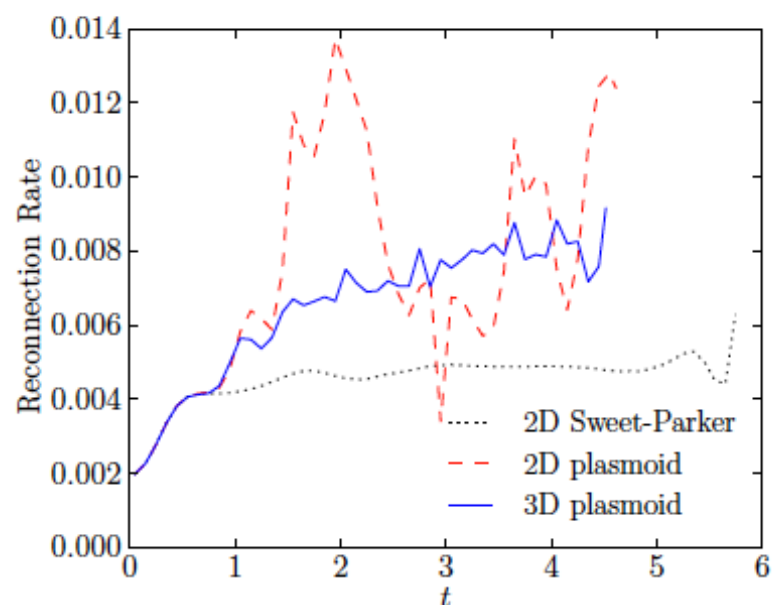
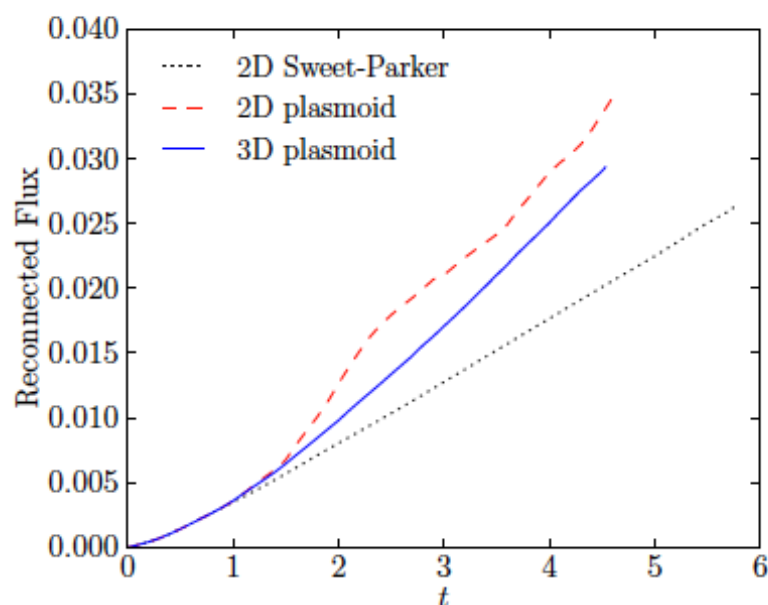


Courtesy: Lijia Guo



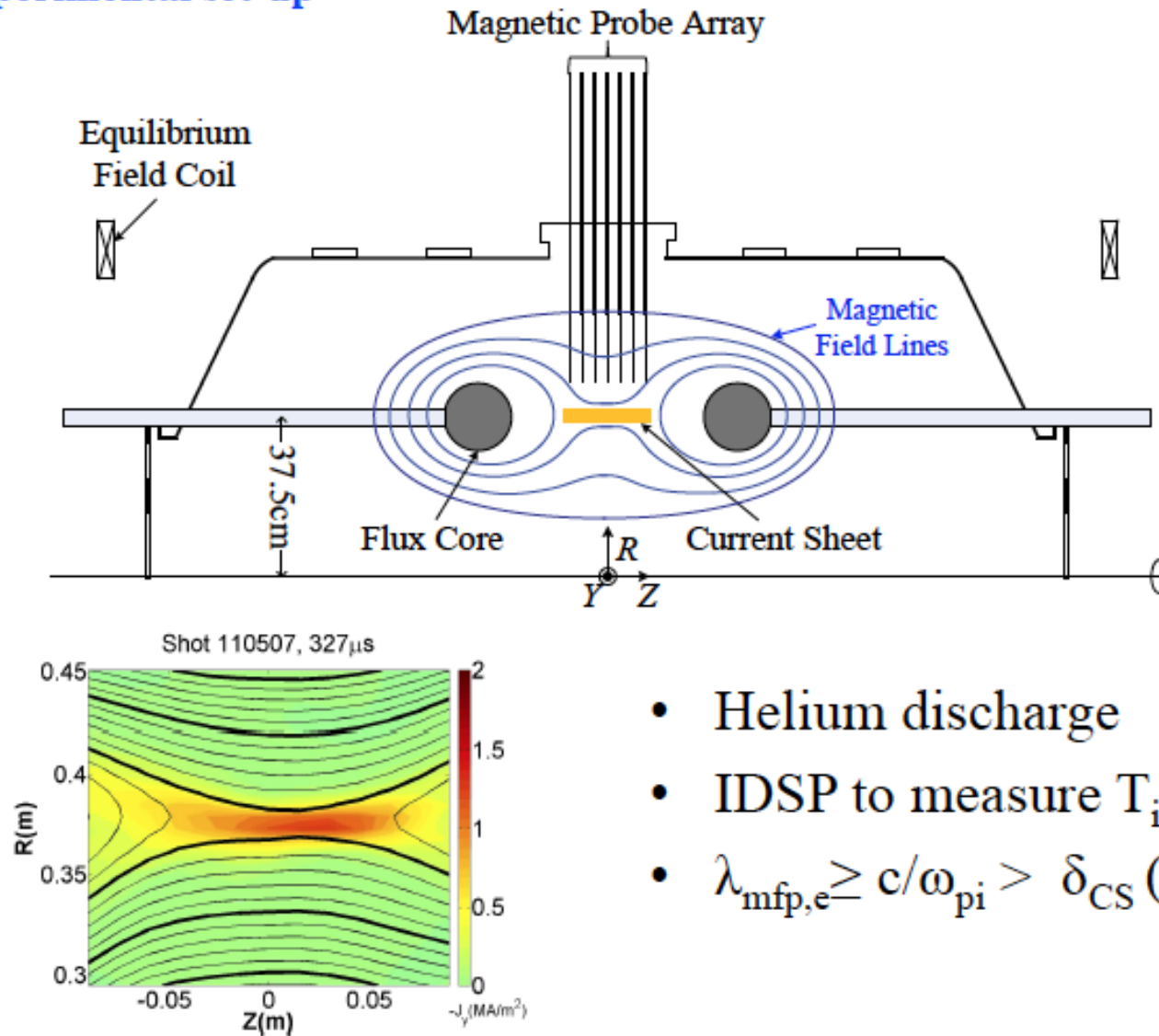
# Reconnection Rate Comparison

- 2D and 3D plasmoid-dominated reconnection achieve comparable, faster than Sweet-Parker, reconnection rate
- 3D reconnection is measured with the mean field  
 $\bar{\mathbf{B}} \equiv \frac{1}{L_z} \int \mathbf{B} dz.$



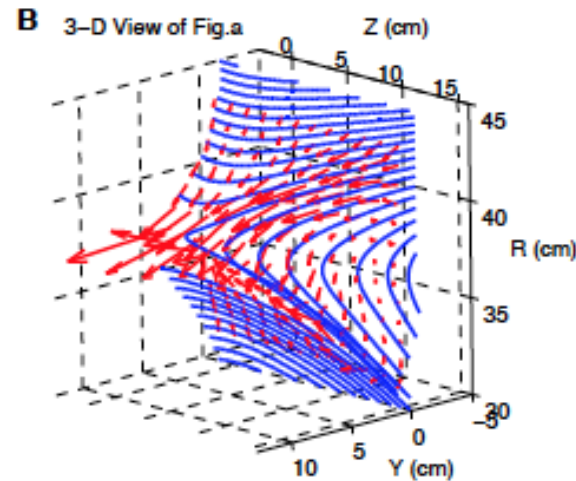
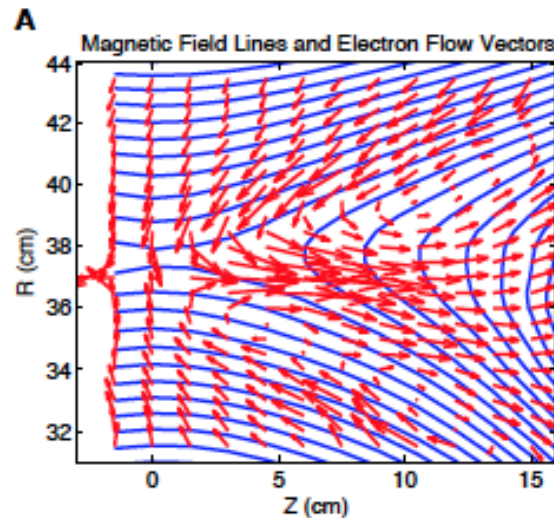
# Energy Conversions: Laboratory Experiment (MRX, PPPL)

## Experimental set-up



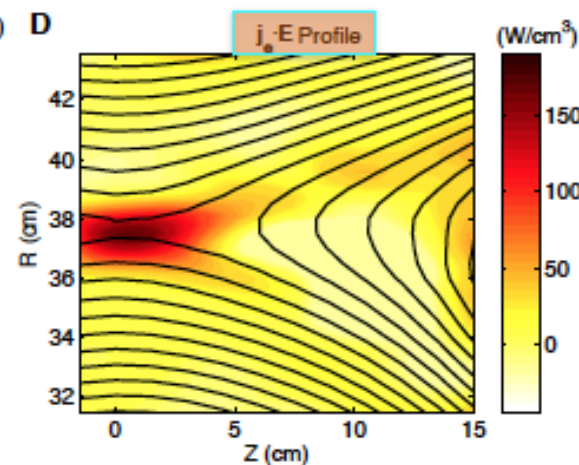
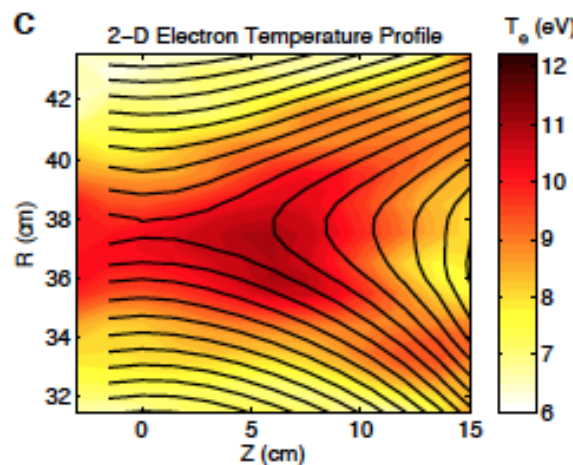
- Helium discharge
- IDSP to measure  $T_i$
- $\lambda_{\text{mfp},e} \geq c/\omega_{pi} > \delta_{CS} (\sim 2\text{cm})$

# Electron dynamics and electron heating in MRX



$$\mathbf{j} = \text{Curl } \mathbf{B}, \quad \mathbf{V}_e = \mathbf{j}_e / n_e$$

Electron gain energy by  $E_y$



- Energy deposition occurs very near the X-point.
- The electron heating seen in wider region through heat conduction

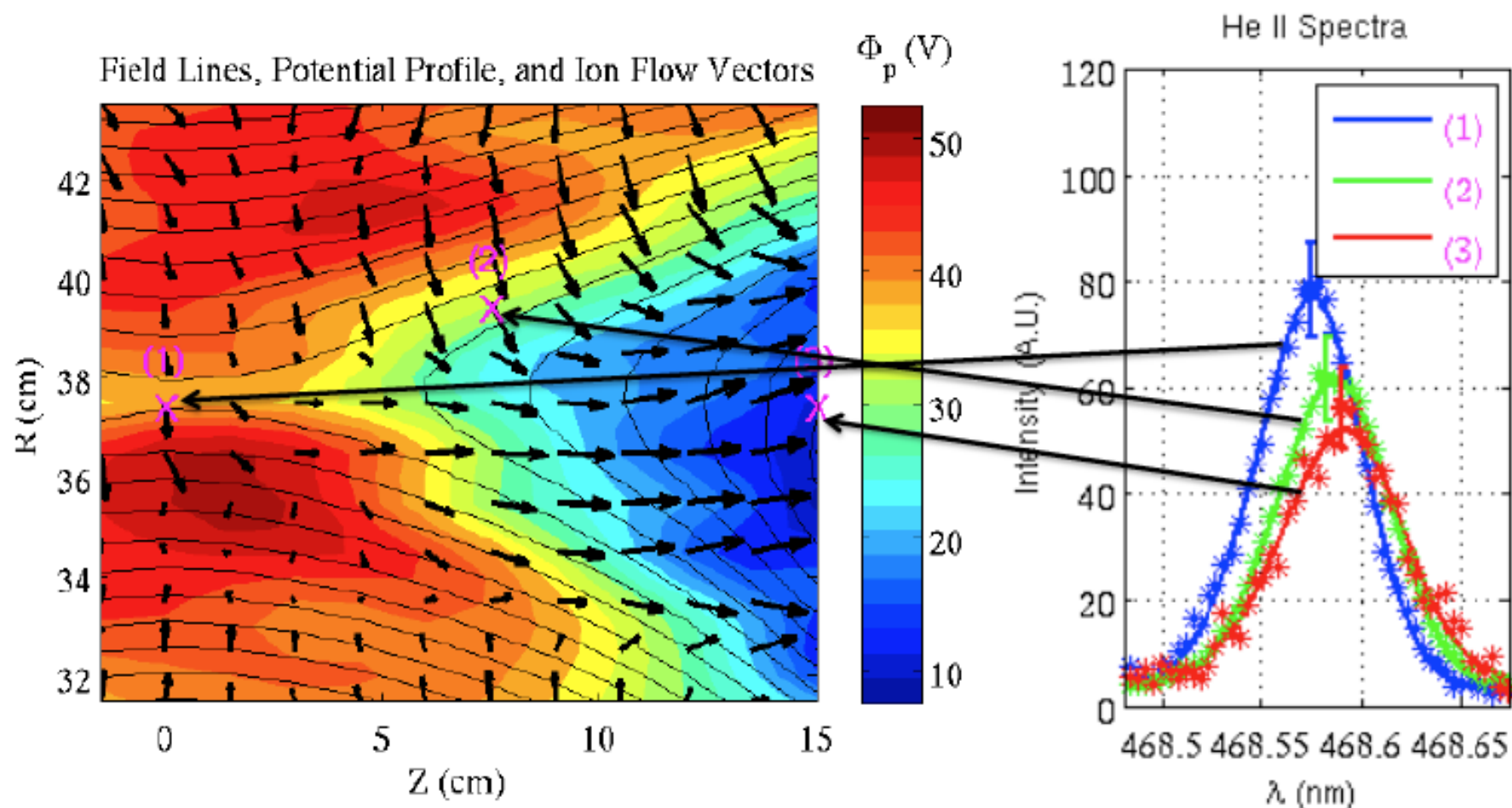
$$j_\perp E_\perp \gg j_\parallel E_\parallel$$

The physics of the high energy deposition rate is not yet resolved.



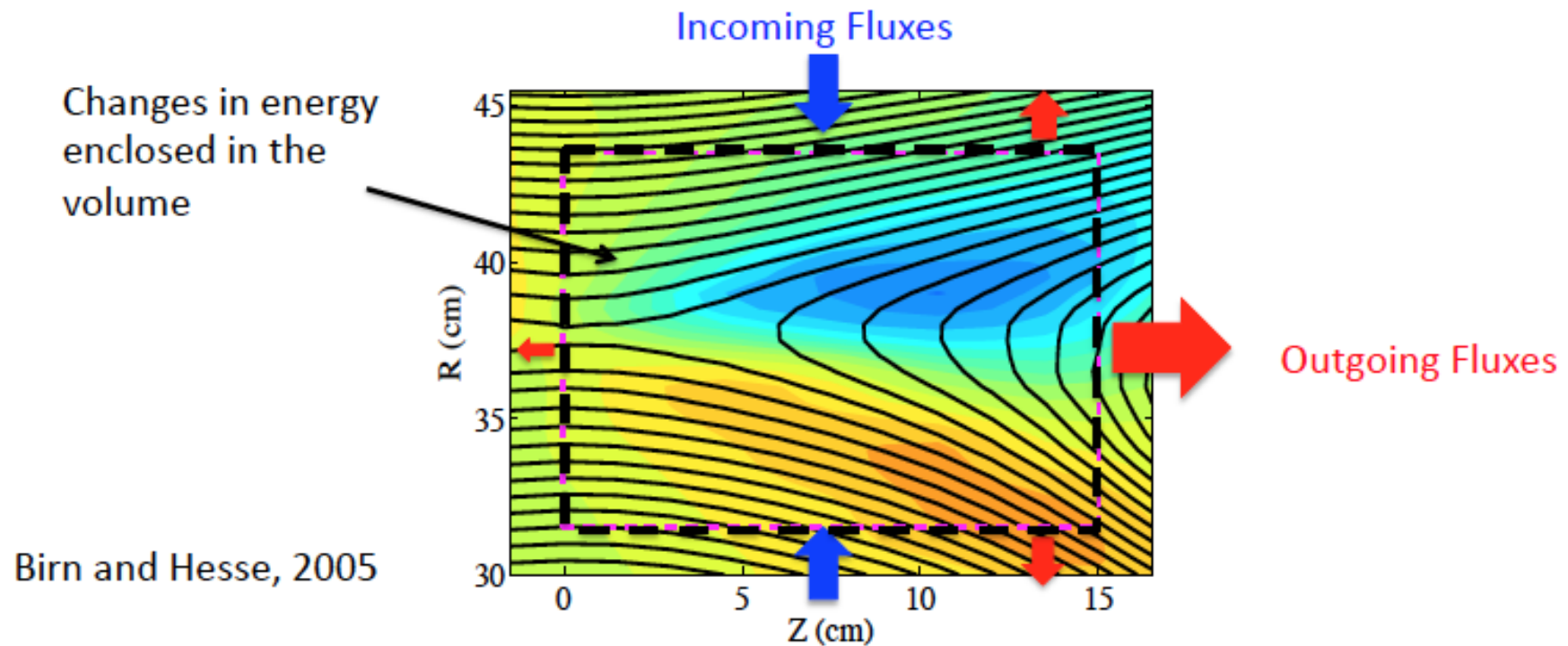


# Ion acceleration and heating in the reconnection layer



Ion heating is attributed to re-magnetization of accelerated ions

# Measurement of energy inventory in MRX

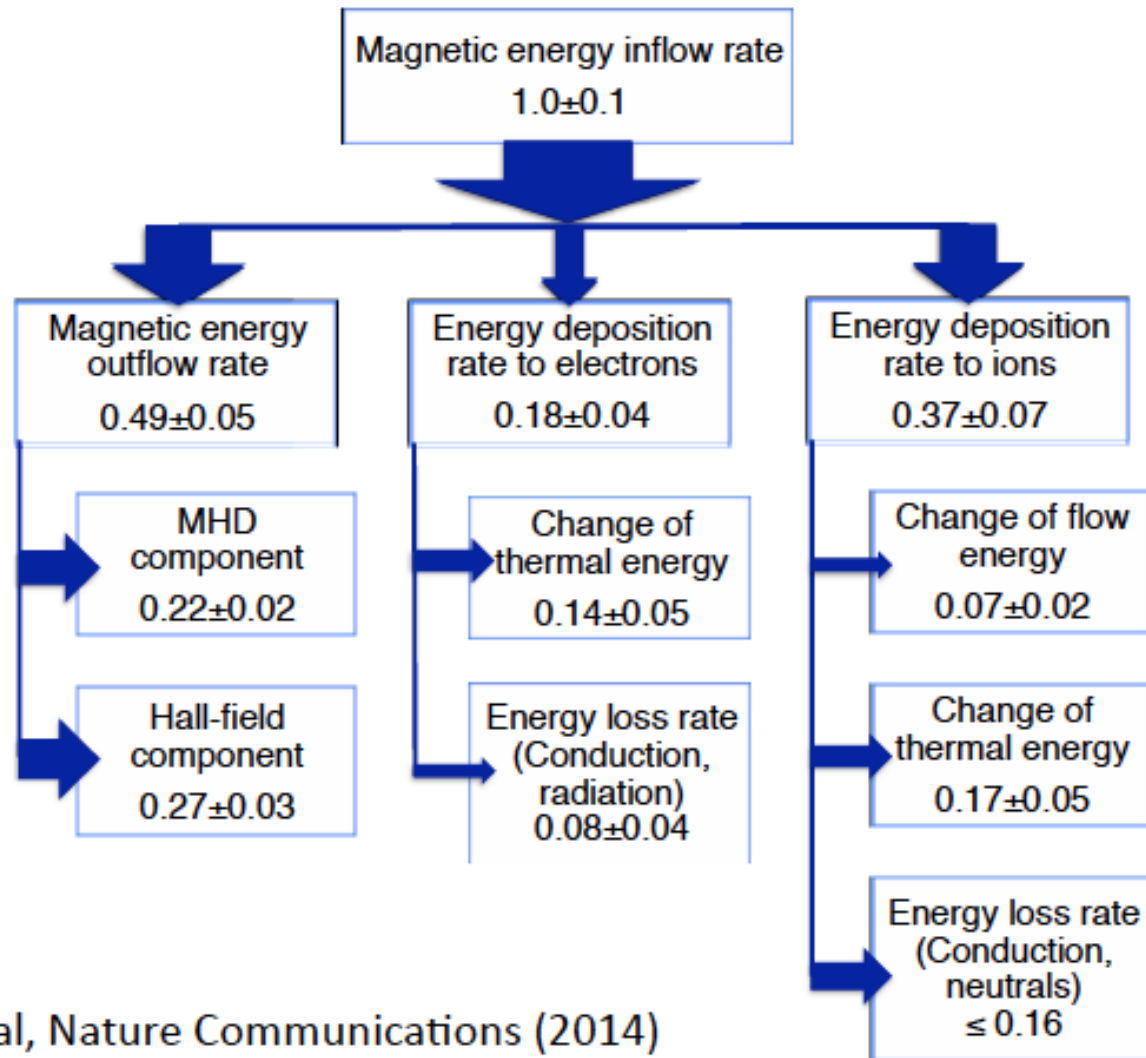


- Energy transport equation :

$$\frac{\partial}{\partial t} \left[ \frac{B^2}{2\mu_0} + \sum_{s=e,i} \left( \frac{3}{2} n_s T_s + \frac{\rho}{2} V_s^2 \right) \right] + \nabla \cdot \left[ \vec{S} + \sum_{s=e,i} \left( \frac{5}{2} n_s T_s \vec{V}_s + \frac{\rho}{2} V_s^2 \vec{V}_s \right) + q_s \right] = 0$$



# Inventory of Energy



Yamada et al, Nature Communications (2014)

## MRX data is compared with simulations and space data

	Magnetic energy Inflow	Magnetic Energy outflow rate	Energy deposition to ions	Energy deposition to electrons
MRX Data	1.0	0.45	0.35	0.20
Numerical simulation	1.0	0.42	0.34	0.22
Magnetotail data (Eastwood)	1.0	0.4	0.39	0.18

- Enthalpy flux dominates in the down flow region
- Magnetic energy outflow substantial

*Energy deposition to ions is generally larger than to electrons.  
With the electrons' heat transport loss is larger than ions',  
 $\Rightarrow T_i \gg T_e$*

# Magnetic Reconnection: Sisyphus of the Plasma Universe



“The struggle itself  
...is enough to fill a  
man’s heart. One  
must imagine  
Sisyphus happy.”  
---Albert Camus in  
*The Myth of  
Sisyphus (Le Myth  
de Sisyphe, 1942)*

*Titian, 1549*